European Journal of Pharmaceutical Sciences 107 (2017) 1–15

Contents lists available at ScienceDirect

European Journal of Pharmaceutical Sciences

journal homepage: www.elsevier.com/locate/ejps

# A novel chalcone derivative, LQFM064, induces breast cancer cells death via p53, p21, KIT and PDGFRA

Bruna Lannuce Silva Cabral[a], Artur Christian Garcia da Silva[a], Renato Ivan de Ávila[a], Alane Pereira Cortez[a], Rangel Magalhães Luzin[b], Luciano Morais Lião[b], Eric de Souza Gil[c], Gérman Sanz[d], Boniek G. Vaz[d], José R. Sabino[e], Ricardo Menegatti[f], Marize Campos Valadares[a,*]

[a] Laboratório de Farmacologia e Toxicologia Celular - FarmaTec, Faculdade de Farmácia, Universidade Federal de Goiás, Goiânia, GO, Brazil
[b] Instituto de Química, Universidade Federal de Goiás, Goiânia, GO, Brazil
[c] Faculdade de Farmácia, Universidade Federal de Goiás, Goiânia, GO, Brazil
[d] Laboratório de Cromatografia e Espectrometria de Massas, Instituto de Química, Universidade Federal de Goiás, Goiânia, GO, Brazil
[e] Instituto de Física, Universidade Federal de Goiás, Goiânia, GO, Brazil
[f] Laboratório de Química Farmacêutica Medicinal (LQFM), Faculdade de Farmácia, Universidade Federal de Goiás, Goiânia, GO, Brazil

ARTICLE INFO

*Keywords:*
Antitumor
Breast cancer
Chalcones
MCF7 cells
Apoptosis

ABSTRACT

This study shows the design, synthesis and antitumoral potential evaluation of a novel chalcone-like compound, (*E*)-3- (3, 5-di-*ter*-butyl-4-hydroxyphenyl)-1- (4-hydroxy-3-methoxyphenyl) prop-2-en-1-one [LQFM064) (**4**)], against human breast adenocarcinoma MCF7 cells. Some toxicological parameters were also investigated. LQFM064) (**4**) exhibited cytotoxic activity against MCF7 cells ($IC_{50}$ = 21 μM), in a concentration dependent-manner, and triggered significant changes in cell morphology and biochemical/molecular parameters, which are suggestive of an apoptosis inductor. LQFM064) (**4**) (21 μM) induced cell cycle arrest at G0/G1 phase with increased p53 and p21 expressions. It was also shown that the compound (**4**) did not interfere directly in p53/MDM2 complexation of MCF7 cells. In these cells, externalization of phosphatidylserine, cytochrome *c* release, increased expression of caspases-7, −8 and −9, reduced mitochondrial membrane potential and ROS over-generation were also detected following LQFM064 (**4**) treatment. Further analysis revealed the activation of both apoptotic pathways via modulation of the proteins involved in the extrinsic and intrinsic pathways with an increase in TNF-R1, Fas-L and Bax levels and a reduction in Bcl-2 expression. Furthermore, KIT proto-oncogene receptor tyrosine kinase, insulin-like growth factor (IGF1) and platelet-derived growth factor receptor A (PDGFRA) were downregulated, while glutathione S-transferase P1 (GSTP1) and interferon regulatory factor 5 (IRF5) expressions were increased by LQFM064 (**4**)-triggered cytotoxic effects in MCF7 cells. Moreover, it can be inferred that compound (**4**) has a moderate acute oral systemic toxicity hazard, since its estimated $LD_{50}$ was 452.50 mg/kg, which classifies it as UN GHS Category 4 (300 mg/kg > $LD_{50}$ < 2000 mg/kg). Furthermore, LQFM064 (**4**) showed a reduced potential myelotoxicity ($IC_{50}$ = 150 μM for mouse bone marrow hematopoietic progenitors). In conclusion, LQFM064 (**4**) was capable of inducing breast cancer cells death via different cytotoxic pathways. Thus, it is a promising alternative for the treatment of neoplasias, especially in terms of the drug resistance development.

## 1. Introduction

Breast cancer, the second most common cancer in the world, frequently diagnosed in women and responsible for millions of new cases registered every year, almost 25% of all cancers (Ferlay et al., 2015), still presents a high mortality rate (Siegel et al., 2016). The current therapeutic approach to this disease involves surgery, radiation therapy, chemotherapy, immune/hormone therapy and targeted therapy. However, the side effects produced by these treatments (e.g. hair loss, gastrointestinal disturbances, neutropenia, and immunosuppression) exert a profound negative impact on health-related quality of life in oncological patients (Nounou et al., 2015). Moreover, the development of tumor resistance to the conventional pharmacological treatment is an enormous obstacle in oncology clinical practice and can lead to treatment failure, disease relapse and death (Velaei et al., 2016). Hence, the urgent need to develop new effective

* Corresponding author at: Faculdade de Farmácia – Universidade Federal de Goiás, Rua 240 esquina com 5ª Avenida, s/n, Setor Universitário, Goiânia, GO 74605.170, Brazil.
*E-mail address:* marizecv@ufg.br (M.C. Valadares).

http://dx.doi.org/10.1016/j.ejps.2017.06.018
Received 7 April 2017; Received in revised form 3 June 2017; Accepted 11 June 2017
Available online 13 June 2017
0928-0987/ 

therapeutic options against breast cancer (Gonzalez-Angulo et al., 2007).

Natural products have been valuable resources for discovery of new anticancer drug candidates (Harvey, 2008; Mahapatra et al., 2015). Due to their structural diversity, chalcones have been widely studied for these purposes (Jandial et al., 2014). However, the obtaining of naturally occurring chalcones, by phytochemical isolation in plants, limits the therapeutic applications of these compounds considering an ecological sustainable approach. To overcome this limitation and even to obtain more effective molecules, design and synthesis of chalcone analogues have demanded great development.

Chalcones are immediate precursors during flavonoid biosynthesis in plants and their structure differs from other members of the family in that they are open-chain analogues. Chemically derived from a common structure, 1,3-diphenyl-2-propene-1-one (**1**), in which two aromatic rings are joined by a three carbon, α-β unsaturated system, with one carbonyl and two carbons (Champelovier et al., 2013; Echeverria et al., 2009). It is well known that the presence of the double bond in conjugation with the carbonyl group is responsible for many of the biological activities of chalcones, such as antimicrobial, anti-inflammatory and anticancer properties (Singh et al., 2014).

Recent studies have also shown the anticancer activity of synthetic chalcone derivatives in a variety of cancer cell lines such as leukemia, colorectal, liver and breast cancers (de Vasconcelos et al., 2013; Maioral et al., 2013; Mohamed et al., 2014; Park et al., 2015; Sharma et al., 2010). In breast cancer cell lines, studies have shown promising cytotoxic activity associated with the inhibition of proliferation, angiogenesis, cell cycle progression, upregulation of tumor suppressors (e.g. p53, p21 and Bax), changes in mitochondrial membrane potential, caspase activation and reactive oxygen species (ROS) overproduction (Lee et al., 2016; Mohamed et al., 2014; Sharma et al., 2010). In addition, other actions at the molecular level related to drug resistance in breast cancer have been described. These include the inhibition of drug efflux transporters, such as P-glycoprotein, and inhibition of the breast cancer resistance protein (Mahapatra et al., 2015).

Given the above, this study describes the obtaining of a new chalcone-like compound, (*E*)-3- (3, 5-di-*ter*-butyl-4-hydroxyphenyl)-1- (4-hydroxy-3-methoxyphenyl) prop-2-en-1-one [LQFM064) (**4**)]. This compound was originally designed and synthesized from molecular hybridization of apocynin (**2**) and butylated hydroxytoluene (BHT) (**3**) using chalcone scaffold (**1**) (Fig. 1). The strategy employed was aimed to improve the anticancer properties found in naturally occurring chalcones, associating antioxidant effects of apocyin (**2**) and BHT (**3**). Moreover, the cytotoxic effects and molecular pathways involved in cell death in MCF7 human breast adenocarcinoma cells as well as some toxicological parameters of LQFM064 (**4**) were investigated.

## 2. Materials and Methods

### 2.1. Chemicals

Roswell Park Memorial Institute (RPMI)-1640 medium, Dulbecco's modified Eagle's medium (DMEM), heat-inactivated fetal bovine serum (FBS), streptomycin/penicillin solution, 3-[4,5-dimethylthiazol-2-yl]-2,5-diphenyl tetrazolium bromide (MTT), granulocyte-macrophage colony-stimulating factor (GM-CSF), propidium iodide (PI), Giemsa dye, RNase, DNase, dichloro-dihydro-fluorescein diacetate (DCFH-DA), rhodamine 123, bovine serum albumin (BSA), RIPA buffer, bicinchoninic acid protein assay kit, protease inhibitor cocktail, thionyl chloride and anhydrous sodium sulfate ($Na_2SO_4$) were purchased from Sigma-Aldrich (St. Louis, MO, USA). Apocynin and formic acid were acquired from Acros Organics (Geel, Belgium), whereas absolute EtOH, dichloromethane ($CH_2Cl_2$), hexane and ethyl acetate were purchased from Neon (Suzano, SP, Brazil). 3,5-di-*tert*-butyl-4-hydroxybenzaldehyde was obtained from Tokyo Chemical Industry (Tokyo, Japan). Annexin V (A) Apoptosis Detection kit FITC, ELISA p53/MDM2 Immunoset kit and CaspaTag™ Caspase-3,-7, -8 and -9 In Situ Assay kit were acquired from eBioscience (San Diego, CA, USA), Enzo Life Sciences (Farmingdale, NY, USA) and Millipore™ (Temecula, CA, USA), respectively. The antibodies against Bax (sc-7480), cytochrome *c* (sc-13561), Fas-L (sc-65400), p21 (sc-6246), p53 (sc-47698) and TNF-R1 (sc-73195) were purchased from Santa Cruz Biotechnology (Santa Cruz, CA, USA). The antibody against Bcl-2 (340575) and BD Cytofix/Cytoperm™ solution were acquired from BD Biosciences (San Jose, CA, USA). MitoTracker® Red CMXRos probe and Hoechst 33,342 were purchased from Invitrogen (Grand Island, NY, USA). Methanol and dimeltilsulfoxide (DMSO) were acquired from Merck (Darmstad, Germany), while Tween 20 was obtained from Vetec (Rio de Janeiro, RJ, Brazil). RNeasy mini kit, RNase-free DNase set and a Human Cancer Drug Targets RT$^2$ Profiler PCR array (PAHS-507) were purchased from Quiagen (Hilden, Germany).

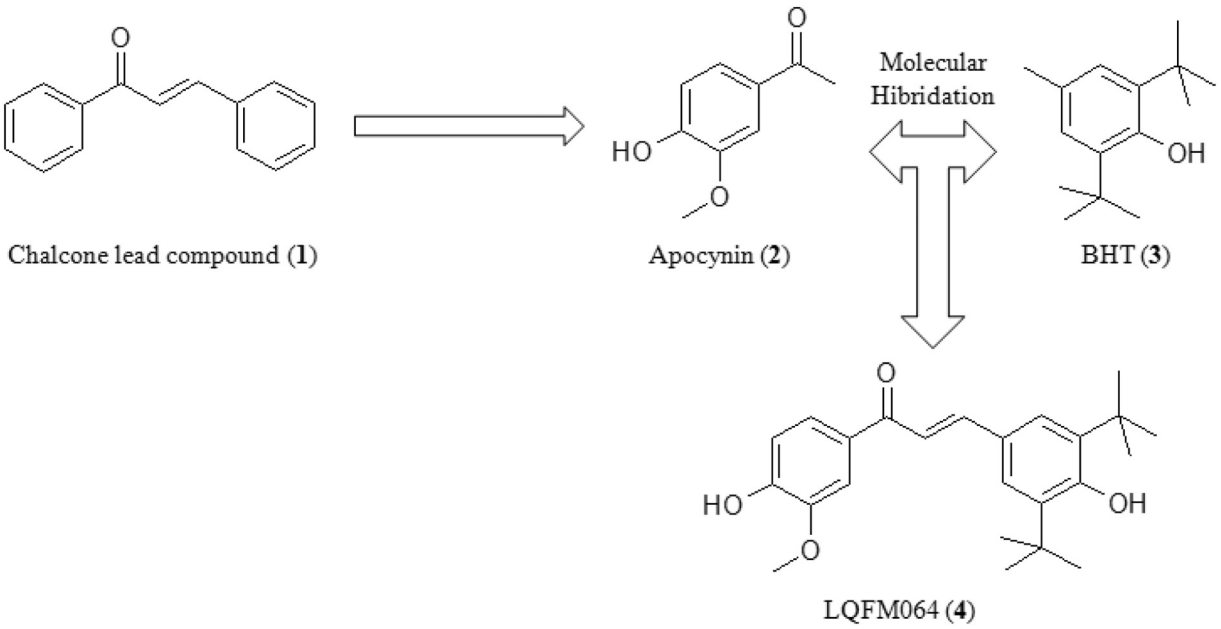


**Fig. 1.** Structural design of LQFM064 (**4**) from molecular hybridization of apocynin (**2**) and butylated hydroxytoluene (BHT) (**3**) using chalcone (**1**) scaffold.

### 2.2. Synthesis of LQFM064 (4)

A total of 0.05 mL (0.5 equiv) of thionyl chloride was added drop by drop to a heterogeneous mixture of apocynin (**2**) (10.0 mmol), 3,5-di-*tert*-butyl-4-hydroxybenzaldehyde (**5**) (10.0 mmol) in 5 mL of absolute EtOH under continuous stirring for 2 h at room temperature. The mixture was then stirred at room temperature for 12 h. After that the EtOH was evaporated and the residue partitioned between water and $CH_2Cl_2$. The organic phase was dried with $Na_2SO_4$, concentrated under vacuum, and the crude product was purified by chromatography using hexane:ethyl acetate as mobile phase to provide LQFM064 (**4**) as a beige solid in a yield of 48%, mp 172–175 °C, Rf = 0.72 ($CH_2Cl_2$/MeOH, 9.5: 5): $IR_{max}$ (KBr) $cm^{-1}$: 3530 ($\nu$ O—H), 3083 ($\nu$ C—H), 2952 ($\nu$ C—H) and 1655 ($\nu$ C═O); $^1H$ NMR (500.13 MHz) $CDCl_3$ $\delta$: 7.78 (1H, d, $J$ = 15.53 Hz, β), 7.64 (1H, dd, $J$ = 8.65 and 1.95 Hz, H-2′), 7.64 (1H, d, $J$ = 1.95 Hz, H-6′), 7.49 (2H, s, H-2 and 6″), 7.38 (1H, d, $J$ = 15.53 Hz, α), 7.00 (1H, d, $J$ = 8.65 Hz, H-3′), 6.24 (1H, 2, H-4′), 5.57 (1H, s, H-4), 3.97 (3H, s, H-5′), 1.48 (18H, s, H-8); $^{13}C$ NMR (125.76 MHz) $CDCl_3$ $\delta$: 189.0 (C-β′), 156.5 (C-4), 150.0 (C-4′), 146.8 (C-5′), 145.3 (C-β), 136.6 (C-3 and 5), 131.5 (C-1′), 126.5 (C-1), 125.9 (C-2 and 6), 123.8 (C-2′), 118.8 (C-α), 113.5 (C-3′), 110.8 (C-6′), 56.3 (C-5′), 34.4 (C-7), 30.3 (C-8); MS: $[M+H]^+$ $m/z$ of 383.2254 (Supplementary Figs. 1-5 and Supplementary Table 1).

Reactions were monitored by TLC using commercially available precoated plates (Whatman 60 F254 silica), and developed plates were examined under UV light (254 and 365 nm). $^1H$ and $^{13}C$ NMR spectra were recorded in the indicated solvent on a Bruker Avance III 500 MHz spectrometer. Chemical shifts are quoted in parts per million downfield from TMS and the coupling constants are in Hertz. Infrared spectra were recorded on a Perkin-Elmer Spectrum Bx-II FT-IR System spectrophotometer instrument as films on KBr discs. Melting points were performed using a Marte melting point apparatus, and the results were uncorrected. All assignments of the signals of $^1H$ and $^{13}C$ NMR spectra are consistent with the chemical structures of the products described. The organic solutions were dried over anhydrous sodium sulfate and organic solvents were removed under reduced pressure in a rotary evaporator. Mass spectrometry analysis was carried out in a microTOF III (Brucker Daltonics, Bremen, Germany) equipped with a commercial ESI (Brucker Daltonics, Bremen, Germany) source set to operate over $m/z$ 100–1500. Samples were extracted using methanol, followed by acidification with 0.1% formic acid. The resulting solution was directly injected with a flow rate of 5 μL·min$^{-1}$. All analyses were performed in the positive mode. ESI(+) source conditions were as follows: nebulizer nitrogen gas temperature and pressure of 2.0 bar and 200 °C, capillary voltage of −4 kV, transfer capillary temperature of 180 °C; drying gas of 4 L·min$^{-1}$; end plate offset of −500 V; skimmer of 35 V and collision voltage of −1.5 V. Each spectrum was acquired using 2 microscans. Mass spectra were acquired and processed with Data Analysis software (Brucker Daltonics, Bremen, Germany). In the X-ray crystallography experiment, a single crystal of the compound (**4**) with a $C_{24}H_{30}O_4$ structural formula suitable for X-ray study, was obtained by slow evaporation of a methanol solution at room temperature. X-ray diffraction data collection was performed using a Kappa Apex II Duo diffractometer with IμS microsource of Mo-Kα radiation. Raw data processing and absorption correction were performed with APEX 2 suite of programs. Structure solution was obtained using Direct Methods implemented in SHELXS[1] and the final refinement was performed with full matrix least squares on $F^2$ using SHELXL[1]. Supplementary Table 2 summarizes the crystal, data collection and refinements. The programs ORTEP-3, SHELXS/SHELXL were used in WinGX software package (Farrugia, 2012; Sheldrick, 2015). The structural data for LQFM064 (**4**) were deposited with the Cambridge Crystallographic Data Centre as Supporting Information, CCDC number: 1513660. Copies of the data can be obtained free of charge upon application to CCDC, 12 Union Road, Cambridge CB2 1EZ, United Kingdom (Fax: (44) 1223 336-033; e-mail: deposit@ccdc.cam.ac.uk). The data related to the chemical

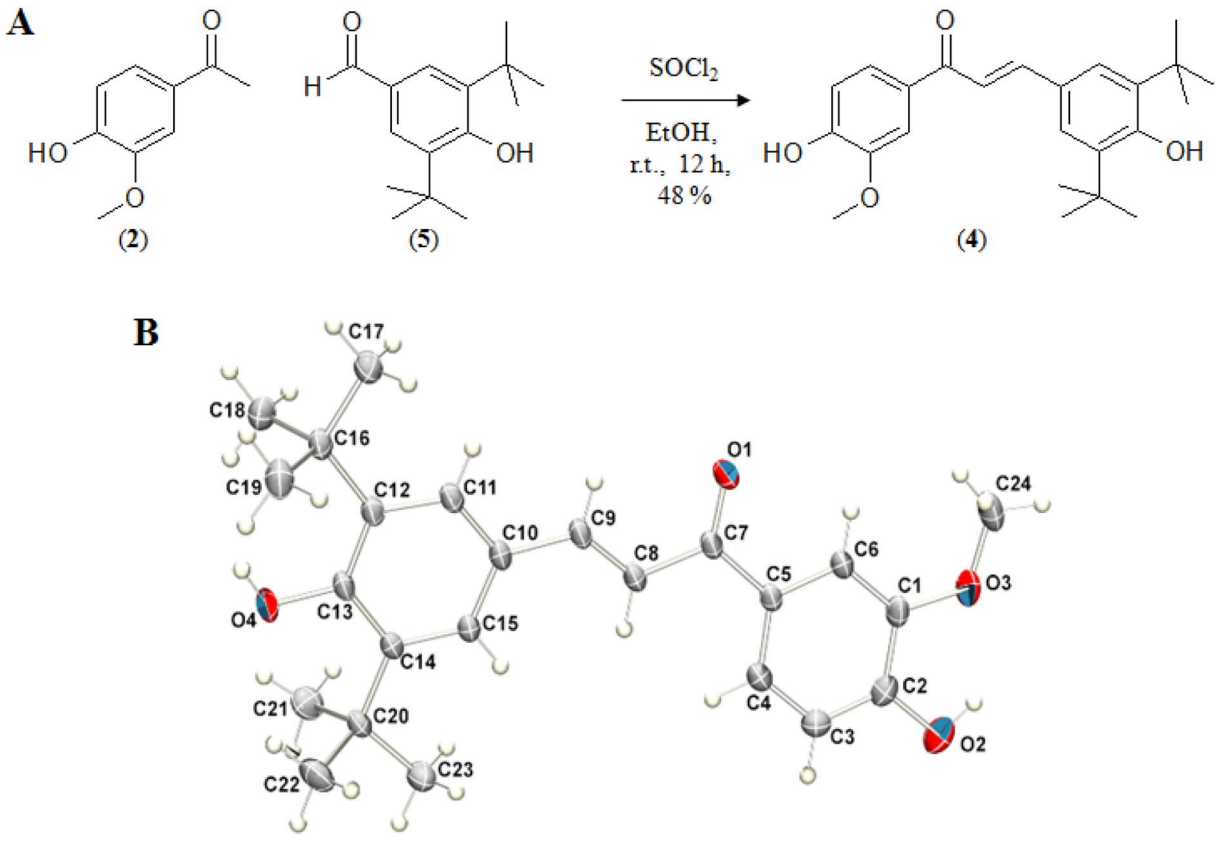


**Fig. 2.** (A) Synthetic route and (B) Ortep view of LQFM064 (**4**).

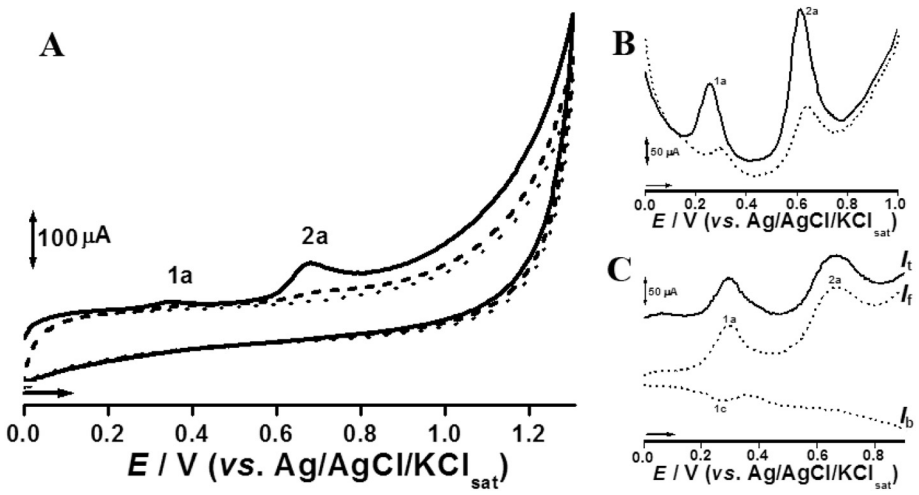


**Fig. 3.** Differential pulse voltammetry (DPV) analysis: **A**) Cyclic B) DP and C) SW voltammograms obtained for LQFM064 (**4**).

characterization of LQFM064 **(4)** are shown in supplementary data (Supplementary Figs. 1–5 and Supplementary Tables 1 and 2).

### 2.3. Differential Pulse Voltammetry (DPV) Analysis

Voltammetric experiments were carried out with a potentiostat/galvanostat µAutolab III® controlled by the GPES 4.9® software (Eco-Chemie, Utrecht, The Netherlands). The measurements were performed with a three-electrode system consisting of a glassy carbon electrode ($d$ = 2 mm), a Pt wire and the Ag/AgCl/KCl (3 M), representing the working electrode, the counter electrode and the reference electrode, respectively. Assays were performed in the potential range of 0 to 1.25 V and at a scan rate of 100 mV $s^{-1}$. The experimental conditions for DPV analysis were as follows: pulse amplitude 50 mV, pulse width 0.5 s and scan rate 10 mV·$s^{-1}$. The square wave voltammetry (SWV) parameters were as follows: pulse 50 mV, frequency 50 Hz and a potential increment of 2 mV, resulting in an effective scan rate of 100 mV$s^{-1}$. The voltammograms were plotted on the software Origin 8® (Northampton, Massachusetts, USA). All experiments were conducted in a 2.0 mL one-compartment electrochemical cell, at room temperature in triplicate ($n$ = 3) and the main electrolyte used was the 0.1 M phosphate buffer (PBS), pH 6.0.

### 2.4. Cell Cultures

Human breast adenocarcinoma MCF7 cells and Balb/c 3T3-A31 fibroblasts were obtained from the Rio de Janeiro Cell Bank (Rio de Janeiro, RJ, Brazil). MCF7 and 3T3 cells were cultured in RPMI-1640 medium and DMEM, respectively, both supplemented with 10% ($v$/v) FBS, penicillin (100 IU/mL) and streptomycin (100 µg/mL). The cell cultures were maintained at 37 °C in a 5% $CO_2$ humidified atmosphere. The cells were passaged three times a week and used in the exponential growth phase. Cell viability was analyzed using a TC20™ automated cell counter (Hercules, CA, USA), according to the manufacturer's instructions. A value > 90% was considered satisfactory for conducting the assays.

### 2.5. Cytotoxicity Assays

#### 2.5.1. MTT Assay

Cell viability evaluation was performed using the MTT reduction test, adapted from Mosmann (1983). Briefly, the cells (1 × $10^5$ cells/mL) were seeded overnight in 96-well plates. They were then treated with eight different concentrations of LQFM064 (**4**) (5–655 µM) for 48 h. Paclitaxel (2–197 µM) was used as a reference drug. After that, 10 µL of MTT (5 mg/mL) were added to each well and the plates incubated for an additional 3 h. Posteriously, the supernatant was discarded and 100 µL of DMSO were added to each well to solubilize the formazan formed. Absorbance was measured at 550 nm using a spectrophotometer (Thermo Scientific Multiskans Spectrum, Boston, MA, USA). Each concentration was tested in six replicates through three independent experiments. Cell viability was expressed as a percentage of the control and $IC_{50}$ values (concentration that inhibited cell growth by 50% compared to untreated group) were obtained. For the subsequent assays, $IC_{25}$ (14 µM) and/or $IC_{50}$ (21 µM) values were used.

#### 2.5.2. Colony Formation Assay

For clonogenic assay, MCF7 cells (2 × $10^3$ cells/dish) were seeded in culture dishes (35 × 10 mm) for overnight. The cells were then treated without or with LQFM064 (**4**) (14 or 21 µM) for 48 h. Posteriously, the cells were washed three times with PBS and fresh complete medium was added in each dish. After 10 days of incubation, the colonies formed were washed with PBS followed by fixation with methanol and staining with Giemsa (10%, v/v) solution. The dishes were photographed and the area (%) occupied by the colonies in each dish was measured using the open-source ImageJ software (http://imagej.nih.gov/ij/).

### 2.6. Morphological Changes Assessment

MCF7 cells (1 × $10^5$ cells/mL) treated with LQM064 (**4**) (21 µM) for 48 h were placed on microscope slides and stained with Giemsa dye. After staining, the slides were examined and photographed under light microscopy (DM 2000, Leica Microsystems, Bannockburn, USA) using a 40 × objective. In addition, nuclear changes were assessed using the Hoechst 33342 DNA binding dye. After incubation, the cells were placed on glass slides, fixed in methanol, permeabilized in PBS containing Tween 20 (0.05%, $v$/v) and incubated with Hoechst 33342 (10 µg/mL) for 20 min at room temperature in the dark. The slides were then washed in PBS and analyzed by fluorescence microscopy (DMI 4000 B, Leica Microsystems, Bannockburn, USA) using a 20 × objective and photographed using the LAS-AF software filter A4 (blue in colour).

### 2.7. Cell Cycle Analysis

MCF7 cells (1 × $10^5$ cells/mL) were treated with LQFM064 (**4**) (21 µM) for 24 and 48 h. After that, the cells were washed with PBS, fixed with ice-cold 70% ethanol and incubated overnight at 4 °C. The cells were then washed twice with PBS and incubated with 300 µL of PBS solution containing RNAse (200 mg/mL) and PI (50 mg/mL) at 37 °C, in the dark, for 1 h. Analysis of fluorescence emitted by the PI–DNA complex was performed using BD FACSCanto II flow cytometer (Becton Dickinson, San Jose, CA, USA) and analyzed by FACSDiva software.

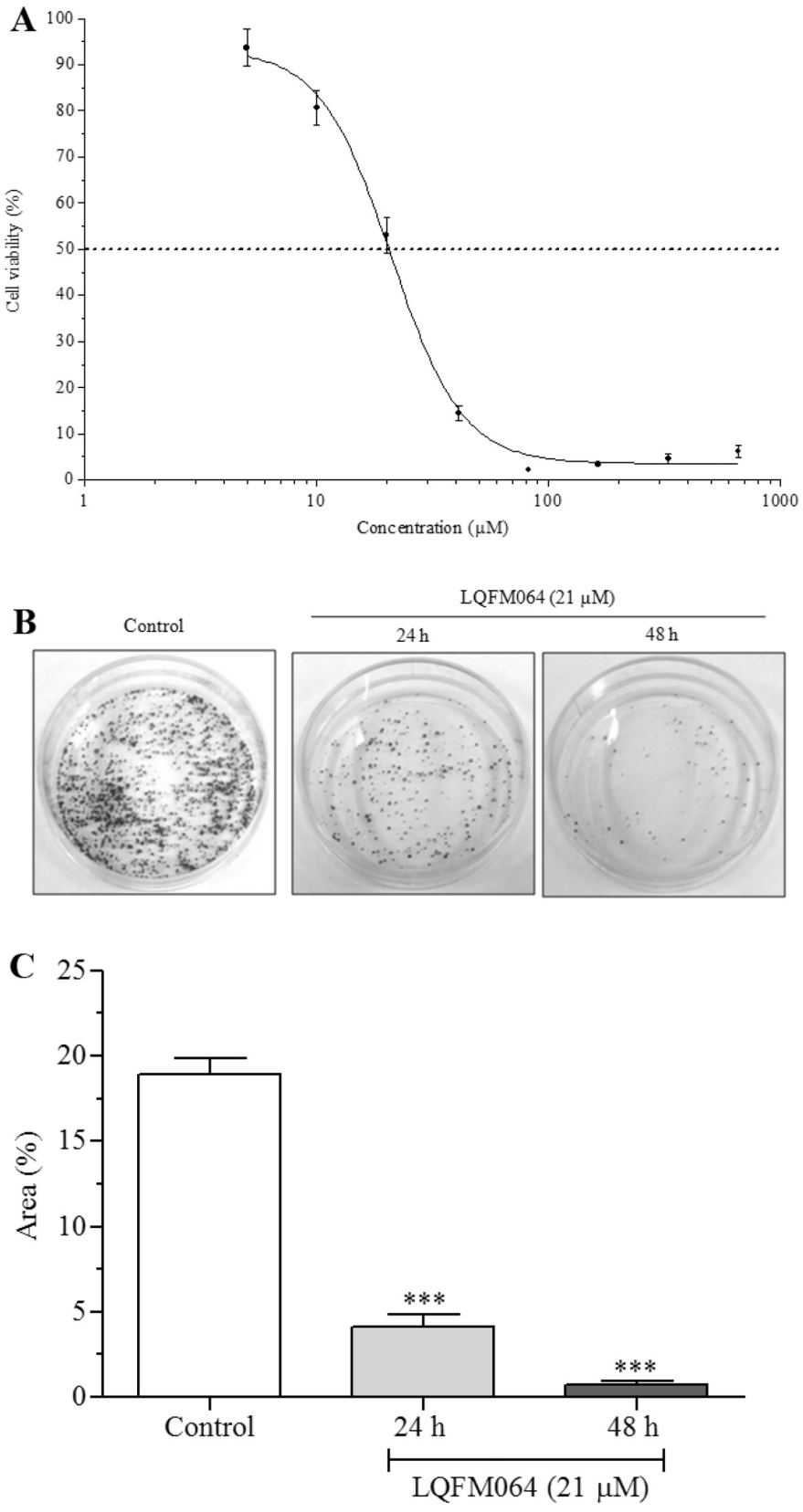


**Fig. 4.** Cytotoxicity evaluation of LQFM064 (**4**) in MCF7 cells. (A) The cells ($1 \times 10^5$ cells/mL) were seeded overnight and then treated with or without different concentrations of LQFM064 (**4**) (5–655 μM) for 48 h. After that, cell viability was evaluated using MTT assay. For clonogenic assay, (B) and (C), MCF7 cells ($2 \times 10^3$ cells/dish) were seeded in culture dishes for overnight. After that, the cells were treated without or with LQFM064 (**4**) (14 or 21 μM) for 48 h followed additional incubation of 10 days. The colonies formed were fixed with methanol and staining with Giemsa solution. The area (%) occupied by the colonies in each dish was then measured. Each point or bar represents mean ± SD of three independent experiments. (***$p < 0.001$ vs. control).

### 2.8. FITC Annexin V/IP Double-Staining and Analysis

Cell apoptosis was assessed by measuring membrane redistribution of phosphatidylserine using an Annexin V (A) Apoptosis Detection kit FITC (eBioscience®), according to the manufacturer's protocol. Briefly, cells ($1 \times 10^5$ cells/mL) were plated and treated with LQFM064 (**4**) (21 μM) for 24 and 48 h. After treatment, MCF7 cells were harvested, washed twice with cold PBS and resuspended in binding buffer (0.1 M Hepes/NaOH, pH 7.4; 1.4 M NaCl and 25 mM $CaCl_2$). The suspensions were transferred to 5 mL tubes and 5 μL FITC Annexin V and 5 μL of PI

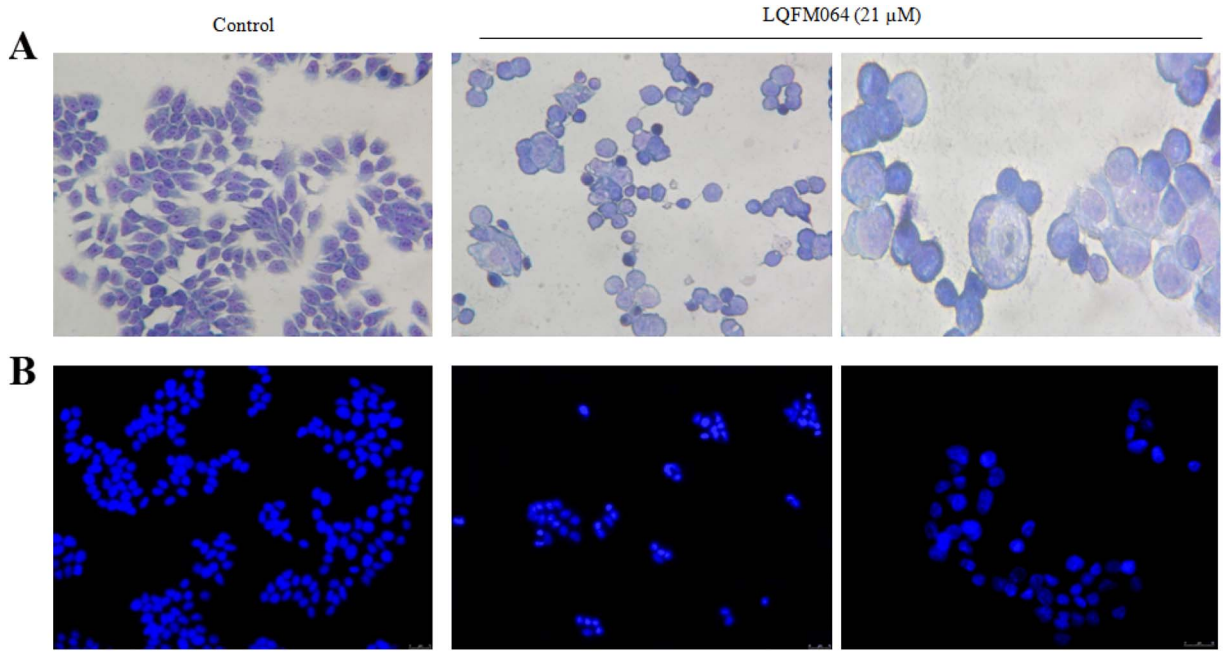


**Fig. 5.** Morphological changes induced by LQFM064 (**4**) in MCF7 cells. The cells ($1 \times 10^5$ cells/mL) were treated with or without LQFM064 (**4**) (21 μM) for 48 h. After that, the cells were then stained with Giemsa dye (A) or Hoechst 33,342 DNA binding dye (B). The images are representative of three independent experiments.

**Table 1**
Genes modulated by LQFM064 (**4**) (14 μM) in MCF7 cells after 48 h treatment.

| Functional gene grouping | Gene | Fold change (control/treated) |
|---|---|---|
| Growth factors & receptors | KIT | − 329.01 |
| | IGF1 | − 72.62 |
| | PDGFRA | − 64.10 |
| | IGF2 | − 7.20 |
| | FLT4 | − 2.59 |
| Drug metabolism | GSTP1 | 2.19 |
| | PTGS2 | − 195.00 |
| Topoisomerases, type II | TOP2A | − 2.70 |
| Histone deacetylases | HDAC7 | − 4.38 |
| | HDAC6 | − 2.53 |
| | HDAC4 | − 2.11 |
| Poly ADP-ribose polymerase | PARP2 | − 2.03 |
| Transcription factors | IRF5 | 2.25 |
| Structural protein | NTN3 | − 5.03 |
| Protein kinases | PLK1 | − 4.95 |

Data are representative of two independent experiments.

were added. The cells were incubated at room temperature for 15 min, after which 400 μL binding buffer were added and analysis was performed in a FACSCanto II flow cytometer. Four cell populations were identified as follows: (1) necrotic cells in the upper-left quadrant (high PI and low FITC signals), (2) early apoptotic cells in the lower-right quadrant (low PI and high FITC signals), (3) late apoptotic cells in the upper-right quadrant (high PI and FITC signals), and (4) viable cells in the lower-left quadrant (low PI and FITC signals).

### 2.9. Caspase Activity

After incubation of MCF7 cells with LQFM064 (**4**) (21 μM) for 24 and 48 h, the active caspases-3/-7, -8 and -9 were assessed by flow cytometer using the CaspaTag™ Caspase In Situ Assay kit (Millipore™, Temecula, CA, USA), in accordance with the manufacturer's instructions.

### 2.10. Evaluation of Mitochondrial Transmembrane Potential (MMP)

The MMP changes were detected by flow cytometer after staining with rhodamine 123, a dye sequestered by active mitochondrias. The MCF7 cells ($1 \times 10^5$ cells/mL) were treated with LQFM064 (**4**) (21 μM) and incubated for 24 h. The cells were then washed with PBS, stained with rhodamine 123 (1 mg/mL) and maintained in the dark for 1 h at 37 °C. The cells were analyzed by a flow cytometer to determine mitochondrial membrane depolarization.

### 2.11. Evaluation of Mitochondrial Activity

Mitochondrial functionality was measured by staining cells with MitoTracker Red, a fluorochrome which measures mitochondrial activity in a MMP-dependent manner. The MCF7 cells ($1 \times 10^5$ cells/mL) were treated with LQFM064 (**4**) (21 μM) and incubated for 24 h. After treatment, the MCF7 cells were washed twice with PBS and incubated with MitoTracker® Red CMXRos (10 nM) in PBS for 15 min at 37 °C in 5% $CO_2$. They were then washed twice, resuspended in 200 μL of PBS and analysis was performed in a flow cytometer.

### 2.12. Cytochrome c Release Analysis

The MCF7 cells ($1 \times 10^5$ cells/mL) were treated with LQFM064 (**4**) (21 μM) and incubated for 24 h. After treatment, the cells were washed twice with PBS-BSA and later fixed and permeabilized with BD Cytofix/Cytoperm™ solution for 20 min at 4 °C. The cells were then washed with PBS-Tween 20 (0.05%, *v*/v) solution and incubated for 20 min with anti-cytochrome *c* antibody. This was followed by washing and analysis in a flow cytometer.

### 2.13. Measurement of Intracellular ROS Overgeneration

Intracellular ROS overproduction was measured by using DCFH-DA fluorimetric probe, which is oxidized to a highly fluorescent compound, 2,7-dichlorofluorescein (DCF), in the presence of ROS. The MCF7 cells ($1 \times 10^5$ cells/mL) were treated with LQFM064 (**4**) (21 μM) and incubated for 24 and 48 h. After treatment, the MCF7 cells were incubated with DCFH-DA (10 μM) at 37 °C in 5% $CO_2$ for 1 h and analyzed in a flow cytometer.

### 2.14. Expression of Proteins Involved in the Process of Cell Death: TNF-R1, Fas-L, Bax, Bcl-2, p53 and p21

Flow cytometer analysis was performed to detect the expression level of the proteins involved in the process of cell death. The MCF7 cells ($1 \times 10^5$ cells/mL) were treated with LQFM064 (**4**) (21 μM) and incubated for 24 and 48 h. After treatment, the MCF7 cells were washed with PBS-BSA and resuspended with BD Cytofix/Cytoperm™ solution for 20 min at 4 °C. The cells were then washed with cold PBS containing Tween 20 (0.05%, v/v) and incubated for 30 min with the antibody against to each protein evaluated. After washing in PBS/BSA (1%, p/v), the cells were resuspended in 400 μL PBS and analyzed in a flow cytometer. For the anti-TNF-R1 and Fas-L antibodies, the permeabilization stage was not performed since these proteins are located in the cytoplasmic membrane.

### 2.15. Quantification of p53-MDM2 Complex

MCF7 cells ($1 \times 10^4$ cells/well) were seeded in 24-well plates and treated with the $IC_{25}$ (14 μM) of LQFM064 (**4**) for 48 h. After treatment, the cells were washed twice with PBS and protein extraction was performed using 200 μL of RIPA buffer containing protease inhibitor cocktail, for 5 min at 4 °C. Cell lysates were stored at − 80 °C to await analysis. Quantification of the p53-MDM2 complex was carried out using the ELISA p53/MDM2 Immunoset kit (Enzo Life Sciences), while the total protein concentration in each sample was determined using the bicinchoninic acid protein assay kit (Sigma-Aldrich), both conducted according to the manufacturer's protocol.

### 2.16. RNA Isolation and Gene Expression Profile

The MCF7 cells ($1 \times 10^5$ cells/mL) were seeded overnight and then treated with or without LQFM064 (**4**) (14 μM) for 48 h. The RNA was then isolated using an RNeasy® Mini kit (Qiagen) following the manufacturer's instructions. The genomic DNA was eliminated using both RNase-free DNase set (Qiagen) and DNase (Sigma) following manufacturer's instructions. Purity of isolated RNA was determined through integrity analysis by agarose gel electrophoresis and measuring ratio of the optical density of the samples at 260/280 nm and 260/230 nm (purity 1.8–2.0) using NanoDrop 8000 spectrophotometer (Thermo Fisher Scientific, Waltham, MA, USA). Complementary DNA strands were synthesized using $RT^2$ First Strand kit (Qiagen, Germany), according to the manufacturer's instructions. 500 μg of total RNA were used from control and treated samples. Pathway-focused gene expression profiling was done using a 96-well Human Cancer Drug Targets, $RT^2$ Profiler PCR array (PAHS-507, Qiagen). In this array, 84 wells contained all the components required for the PCR reaction in addition to a primer for a single gene in each well. Real-time PCR was performed using the Rotor Gene Q, by heating the plate at 95 °C for 10 min, followed by 40 cycles at 95 °C for 15 s and 60 °C for 30 s. Data analysis was performed using the ΔΔCt method (delta delta cycle threshold); the analysis was performed automatically according to the SABiosciences company (Qiagen, USA) web portal (www.SABiosciences.com/pcrarraydataanalysis.php). Changes in gene expression were illustrated as a fold increase or decrease. The data were normalized, across all plates, to the following housekeeping genes provided by kit and the data were obtained by duplicate arrays.

### 2.17. 3T3 Neutral Red Uptake (NRU) Assay

Evaluation of the cytotoxicity of LQFM064 (**4**) to 3T3 cells was performed according to the standard protocol of Borenfreund and Puerner (1985), modified by ICCVAM (2006). Briefly, 3T3 cells ($3 \times 10^4$ cells/well) were seeded in 96-well plates overnight. The cells were then treated with eight different concentrations of LQFM064 (**4**) (5–655 μM) for 48 h. Paclitaxel (0.02–2 μM) was used as a reference drug. After that, the solutions were removed from the plates and 100 μL of DMEM containing 5% (v/v) FBS and neutral red (NR, 0.25 mg/mL) were added to each well. After 3 h incubation, the NR medium was discarded and the cells washed with PBS. The PBS was decanted from the plate and 100 μL of NR desorb solution (50 EtOH: 1 acetic acid: 49 water) were added to all wells. The plates were shaken and absorbance was measured at 550 nm using a spectrophotometer (Thermo Scientific Multiskans Spectrum, Boston, MA, USA). Each concentration was tested in six replicates through three independent experiments. Cell viability was expressed as a percentage of the control and $IC_{50}$ value was obtained and used to estimate the $LD_{50}$ (median lethal dose), based on the equation of the *in house* model previously established by Vieira et al. (2011): $\text{Log } (LD_{50}) = 0.545 \times \log (IC_{50}) + 0.757$. The estimated $LD_{50}$ value was then used to classify the probable acute oral systemic toxicity of LQFM064 (**4**) according to the United Nations Globally Harmonized System of Classification and Labelling of Chemicals (UN GHS).

### 2.18. Investigation of Potential Myelotoxicity of LQFM064 (4)

Potential myelotoxicity of LQFM064 (**4**) was performed by the colony-forming unit-granulocyte macrophage (CFU-GM) clonogenic assay in mouse bone marrow cells. Bone marrow cells from a mouse were aseptically collected, transferred to a sterile plastic tube containing RPMI, and centrifuged at 1500 rpm for 10 min. After that $1 \times 10^5$ cells/mL were seeded in Petri dishes (35 × 10 mm), maintained in 2 mL of 2 × DMEM containing 20% (v/v) FBS, 50% (*v*/v) agar (0.6%, p/v), GM-CSF (0.5 ng/mL) with or without six different concentrations of LQFM064 (**4**) (5–164 μM). The plates were incubated for 7 days in a fully humidified atmosphere of 5% $CO_2$ in air at 37 °C. Colony formation (clones > 50 cells) was scored at 35 × magnification using a dissection microscope (Leica, Germany). Each concentration was tested in three independent experiments in three replicates. Paclitaxel (0.018 μM) was used as a positive control, according to Pessina et al. (2001).

### 2.19. Statistical Analysis

The assays were carried out in two or three independent experiments. The cytotoxicity results, expressed as the mean ± SD of six replicates, were transformed into percentages of the control and $IC_{25}$ and $IC_{50}$ values were obtained by non-linear regression. For flow cytometer analysis, 10,000 events were collected per sample of each assay using a BD FACSCanto II flow cytometer. The difference between control and LQFM064 (**4**)-treated cells was evaluated by unpaired *t*-test or one-/two-way analysis of variance (ANOVA) followed by Bonferroni's test using GraphPad Prism version 5.01 software for Windows (San Diego, CA, USA). Statistical significance was established as $p < 0.05$.

## 3. Results

### 3.1. Synthesis of LQFM064 (4)

As illustrated in Fig. 2A, LQFM064 (**4**) was obtained, using chalcone as scaffold, through a cheap and relatively easy sustainable synthesis process by aldol condensation between apocynin (**2**) and 3,5-di-*tert*-butyl-4-hydroxybenzaldehyde (**5**), catalysed by thionyl chloride, in 48% yield. Fig. 2B shows ortep view of the LQFM064 (**4**).

### 3.2. Analysis of Antioxidant Potential of LQFM064 (4)

Electrochemical characterization was carried out using DPV analysis to evaluate the electron donor character and stability to oxidation of LQFM064 (**4**). The free phenolic groups were electrochemically oxidized at glassy carbon electrode, and exhibited two anodic peaks 1a and 2a at peak potentials Ep1a = 0.3 V and Ep2a = 0.7 V, respectively. On successive scans, a strong adsorption character was seen, leading to

electrode passivation and, as a consequence, peak current-decay (Fig. 3A and B). The low peak potential, related to the anodic process (1a), is consistent with species with high reducing power. Moreover, the SWV experiments exhibited a certain reversible character for redox process 1a/1c, which is also consistent with promising antioxidants.

### 3.3. Cytotoxicity Analysis

In MTT assay, it was verified that the proliferation of MCF7 cells was inhibited by LQFM064 (**4**) (5–655 μM) in a concentration dependent-manner (Fig. 4A). The $IC_{50}$ value obtained was 21 μM, similarly to that found for paclitaxel ($IC_{50}$ = 23.2 μM) (data not shown). In addition, colony formation assay showed that the cells treated with LQFM064 (**4**) (14 or 21 μM) for 48 h had low proliferative activity after 10 days (Fig. 4B). This reduction in number of colonies formed was concentration-dependent manner. The area occupied by the treated cells in each dish was significantly reduced ($p < 0.001$) in comparison to control (Fig. 4C).

### 3.4. Effects of LQFM064 (4) in Cell Morphology of MCF7 Cells

The treatment of MCF7 cells with LQFM064 (**4**) (21 μM) led to pronounced changes in cell morphology, such as cell shrinkage and pyknosis, formation of cytoplasmic vacuoles and chromatin condensation, when compared with untreated cells (Fig. 5A). In addition, Hoescht 33342 staining analysis showed that nuclei broken into fragments were seen with consequent low fluorescence, as well as chromatin condensation and pleomorphic nuclei, in contrast to untreated cells (Fig. 5B). When all these are considered, the LQFM064 (**4**)-induced morphological changes are suggestive features of apoptotic cell death.

### 3.5. Effects of LQFM064 (4) on Cell Cycle Progression

As regards cell cycle progression in MCF7 cells, LQFM064 (**4**) significantly promoted an increase of 8.57% ($p < 0.01$) and 13.13% ($p < 0.001$) in the number of cells at G0/G1 phase after 24 and 48 h of treatment, respectively. Therefore, a significant reduction of 9.77% and 10.87% was detected at S phase ($p < 0.001$) for the above-mentioned exposure times (Fig. 6A and B). These results suggest that LQFM064 (**4**) reduced the MCF7 cells proliferation associated with cell cycle arrest in the G0/G1 phase.

### 3.6. Phosphatidylserine (PS) Exposure Induced by LQFM064 (4)

Loss of plasma membrane asymmetry by PS exposure in MCF7 cells treated with or without LQFM064 (**4**) was evaluated by A/PI double-staining. As expected, untreated cells showed high viability rate (A-/PI- cells) (96.35 ± 1.7%). By contrast, cells treated with LQFM064 (**4**) showed a significant reduction in viability in a time-dependent manner as follows: viable (62.4 ± 0.28%, A-/PI-) ($p < 0.001$), early apoptotic (6.9 ± 1.8%, A+/PI-), late apoptotic (14.8 ± 1.6%, A+/PI+) ($p < 0.01$) and necrotic (15.85 ± 3.8%, A-/PI+) ($p < 0.001$) cells after 24 h exposure and viable (50.6 ± 6.0%, A-/PI-) ($p < 0.001$), early apoptotic (14.25 ± 0.2%, A+/PI) ($p < 0.01$), late apoptotic (17.45 ± 1.0%, A+/PI+) ($p < 0.001$) and necrotic (17.75 ± 5.1%, A-/PI+) ($p < 0.001$) cells after 48 h of treatment (Figs. 7A and B).

### 3.7. Involvement of caspases in LQFM064 (4) induced apoptosis

Flow cytometry analysis showed that caspase activities were significantly increased during the LQFM064 (**4**)-induced cell death (Fig. 8). When the cells were treated with LQFM064 (**4**) for 24 h, it was verified an increase of 13.4% ($p < 0.001$), 10.82% ($p < 0.01$) and 15.55% ($p < 0.001$) in the activities of caspase-3/-7, -8 and -9, respectively; while this increase was 12.17% ($p < 0.01$), 13.82% ($p < 0.001$) and 11.05% ($p < 0.01$) when the cells were treated for 48 h.

### 3.8. Mitochondrial Dysfunction Promoted by LQFM064 (4)

Considering that alterations in mitochondrial function are one of the early events in apoptosis, the effects in the MMP were investigated after 24 h of exposure to LQFM064 (**4**). Mitochondrial assessment showed that the LQFM064 (**4**) promoted a loss of 33.27% ($p < 0.01$) of MMP (Fig. 9A). LQM064 (**4**) also promoted a significant reduction in mitochondrial activity due to a decrease of 17.77% ($p < 0.001$) using MitoTracker Red staining, when compared to untreated cells (Fig. 9B). Moreover, a significant accumulation of cytosolic cytochrome *c* induced by LQFM064 (**4**) was shown ($p < 0.01$) in contrast to untreated cells (Fig. 9C). These findings show that a mitochondria-dependent pathway could contribute to LQFM064 (**4**)-induced apoptosis in MCF7 cells.

### 3.9. ROS Overproduction is Involved in Apoptosis Induced by LQFM064 (4)

A time-dependent overgeneration of ROS after 24 and 48 h of treatment with LQFM064 (**4**) was seen. As shown in Fig. 10, there was a marked increase in the generation of ROS depending on incubation time. Cells treated with LQFM064 (**4**) for 24 h increased ROS by 78.25% and reached up to 333% ($p < 0.05$) at 48 h.

### 3.10. Modulation of Proteins Involved in the Process of Apoptosis

The effects of LQFM064 (**4**) on the role of signaling molecules involved in apoptosis, such as TNF-R1, Fas-L, Bax, Bcl-2, p53 and p21, were investigated (Fig. 11). It is known that TNF-R1 and Fas-L are extensively analyzed in the cascade of events involved in the activation of the extrinsic pathway of apoptosis. In this study, treatment of MCF7 cells with LQFM064 (**4**) induced an increase in the expression of both proteins. The expression of TNF-R1 and Fas-L increased by 25.67 ($p < 0.001$) and 44.65% in 24 h, respectively, in comparison to control. After 48 h of treatment, TNF-R1 expression increased by 59.75% ($p < 0.001$), while the Fas-L expression was not statistically significant. The results of the Bax expression in MCF7 cells after treatment with LQFM064 (**4**) showed a considerable increase of 140.6% ($p < 0.01$) and 262.8% ($p < 0.001$) after 24 and 48 h, respectively; whereas Bcl-2 protein showed a progressive reduction in levels, 24.15% ($p < 0.01$) and 46.20% ($p < 0.001$) after 24 and 48 h of treatment, respectively. As regards the proteins involved in cell cycle progression, treatment with LQFM064 (**4**) for 24 h caused an increase of 69.80% ($p < 0.01$) in p53 expression, while after 48 h there were no significant changes. In p21 expression analysis, increases of 5.23% and 67.07% ($p < 0.05$) were seen after 24 and 48 h of treatment, respectively.

### 3.11. Quantification of the p53-MDM2 Complex

As shown in Fig. 12, LQFM064 (**4**) treatment for 48 h did not alter the intracellular amounts of the p53/MDM2 complex in MCF7 cells, which indicates that the compound did not directly interfere in the p53/MDM2 complexation.

### 3.12. Cellular Gene Expression After LQFM064 (4) Treatment

In order to identify the gene modulation triggered by the LQFM064 (**4**), several genes associated with oncogenesis as well as possible targets for anticancer therapeutics were investigated using the Human Cancer Drug Targets $RT^2$ Profiler PCR array (Quiagen) through the qPCR. From the 84 genes analyzed, 15 genes were modulated by the treatment with LQFM064 (**4**), most of them were downregulated, and 2 genes were upregulated (Fig. 13 and Table 1). KIT proto-oncogene receptor tyrosine kinase, insulin-like growth factor (IGF1) and platelet-derived growth factor receptor A (PDGFRA) expression was extensively

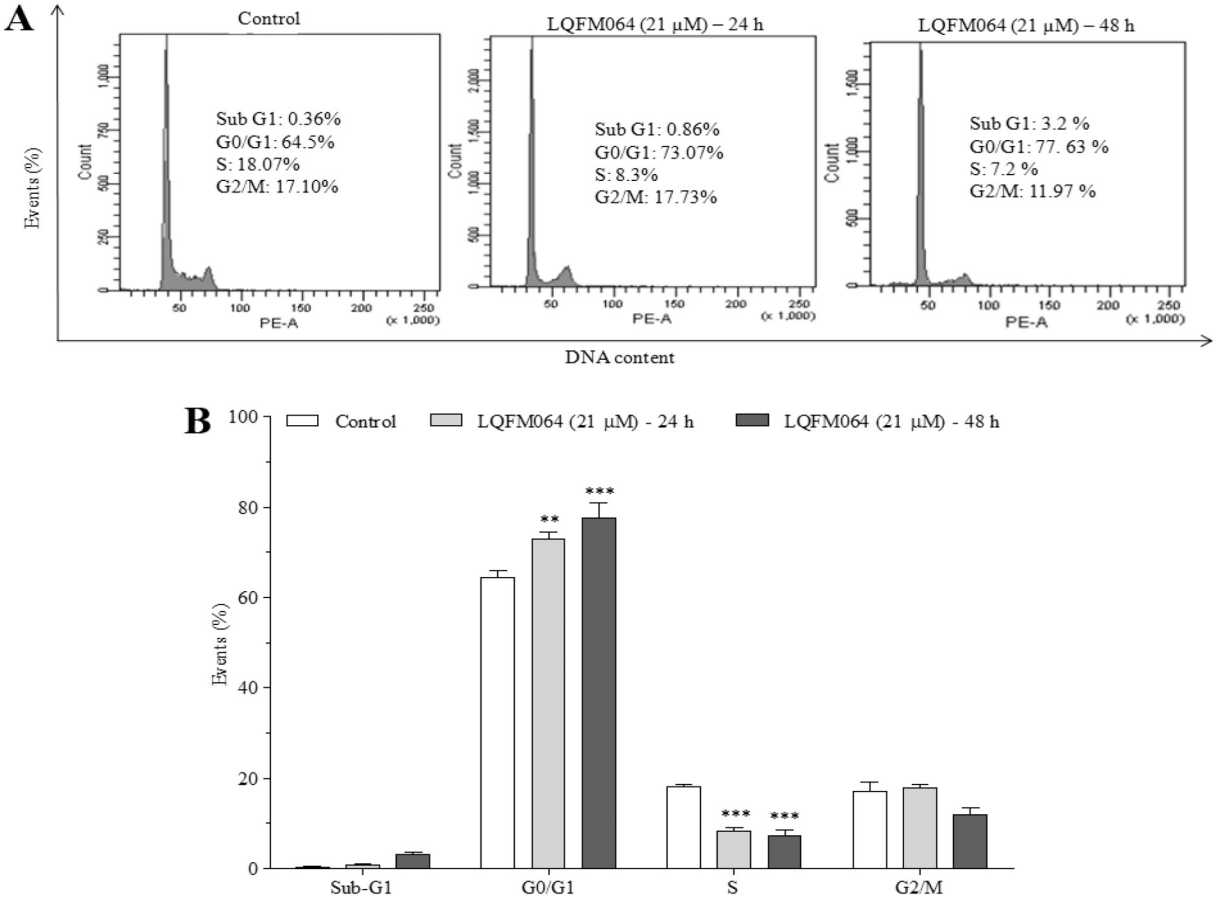


**Fig. 6.** Effects of LQFM064 (**4**) in the cell cycle of MCF7 cells. (A) Representative histograms of the analysis of cell cycle in MCF7 cells following 24 and 48 h of treatment with or without LQFM064(**4**) (21 µM). (B) Effects of LQFM064 (**4**) in cell cycle progression, presented as the percentage of cells, at sub G1, G0/G1, S and G2/M phases. Each bar represents the mean ± SD of three independent experiments. (**$p < 0.01$ and ***$p < 0.001$ vs. control).

decreased, > 50 fold change, after MCF7 cell treatment with LQFM064 (**4**). While Glutathione S-transferase P1 (GSTP1) and interferon regulatory factor 5 (IRF5) expressions were two fold increased.

### 3.13. 3T3 NRU Assay

The cytotoxic effects of the eight concentrations of LQFM064 (**4**) (5–655 µM) on Balb/c 3T3-A31 cells by NRU assay are shown in Fig. 14. The proliferation of these cells was inhibited by LQFM064 (**4**) in a concentration-dependent manner. The $IC_{50}$ obtained was 30 µM, whereas this value was 0.105 µM for paclitaxel (data not shown). Using these findings as a basis, $LD_{50}$ was estimated and the value found was 452.50 mg/kg. Therefore, LQFM0064 (**4**) was classified at UN GHS category 4 (300 mg/kg > $LD_{50}$ < 2000 mg/kg).

### 3.14. Potential myelotoxicity evaluation of LQFM064 (4)

The effects of LQFM064 (**4**) on mouse bone marrow granulocyte/macrophage progenitor cells are presented in Fig. 15. As expected, paclitaxel (0.018 µM) significantly decrease the bone marrow progenitor cells ($p < 0.001$), whereas LQFM064 (**4**) exposure did not significantly change the number of bone marrow CFU-GM at concentrations of 5, 10, 20 or 41 µM when compared to the control. On the other hand, higher concentrations of LQFM064 (**4**) (82 and 164 µM) produced a reduction in the number of colonies ($p < 0.01$). The $IC_{50}$ value obtained was 150 µM. Although LQFM064 (**4**) reduced the viability of mouse bone marrow hematopoietic progenitors, it is interesting to mention that paclitaxel was more cytotoxic in comparison to LQFM064 (**4**). In addition, its $IC_{50}$ obtained was seven times higher than that value found in MCF7 breast cancer cell line. These findings could suggest that the LQFM064 (**4**) has a reduced potential hematoxicity.

## 4. Discussion

In this study, we described the design, synthesis and cell death molecular pathways of the new chalcone analogue LQFM064 (**4**) against MCF7 breast cancer cells. The results showed that this compound (**4**) inhibited MCF7 cells growth by inducing cell cycle arrest at G0/G1 phase, probably associated with increase in p53 and p21 expressions. However, the effects on p53 were not due to a direct effect on p53/MDM2 complexation. The mechanisms of cell death investigated suggested the induction of apoptosis via intrinsic and extrinsic pathways by LQFM064 (**4**). After the treatment, the MCF7 cells showed morphology of apoptosis associated with loss of plasma membrane asymmetry by PS exposure. Moreover, we also observed an increase in caspase-3/-7, -8 and -9 activities. Considering that this cell line did not express caspase-3 (Jänicke, 2009), the increase found was probably related to caspase-7. Furthermore, accumulation of cytosolic cytochrome *c*, mitochondrial dysfunction and ROS overgeneration were detected after treatment with LQFM064 (**4**). In terms of the modulation of proteins related to apoptosis, LQFM064 (**4**) triggered an increase in TNF-R1, Fas-L and Bax and a reduction in Bcl-2 expression. Furthermore, this compound (**4**) showed antioxidant properties. In order to investigate the molecular mechanisms induced by LQFM064 (**4**), a gene expression array profile was performed. Despite the most of 84 genes expression analyzed were not changed after LQFM064 (**4**) treatment, KIT, PDGFRA and IGF1 revealed downregulated.

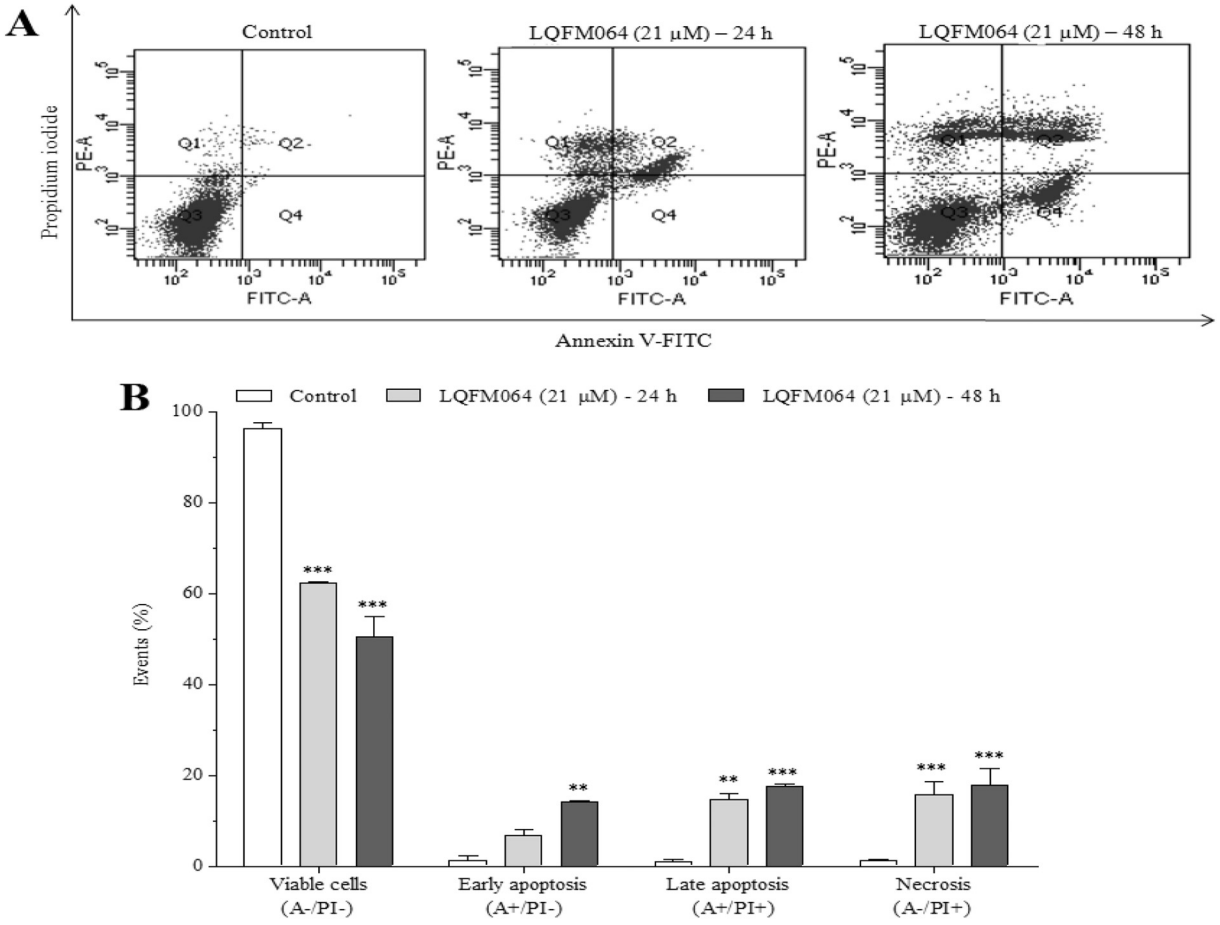


**Fig. 7.** Phosphatidylserine (PS) externalization analysis in MCF7 cells treated with or without LQFM064 (**4**). The cells ($1 \times 10^5$ cells/mL) were seeded overnight and then treated with or without LQFM064 (**4**) (21 μM) for 24 and 48 h. After that, the cells were stained with FITC Annexin V (A)/iodide propidium (IP) and analyzed using flow cytometer. (A) Representative histograms of PS externalization analysis. Four cell populations are shown as follows: (1) necrotic cells in the upper-left quadrant (high PI and low FITC signals); (2) early apoptotic cells in the lower-right quadrant (low PI and high FITC signals); (3) late apoptotic cells in the upper-right quadrant (high PI and FITC signals); and (4) viable cells in the lower-left quadrant (low PI and FITC signals). (B) Percentage of viable, early apoptotic, late apoptotic and necrotic cells. Each bar represents the mean ± SD of three independent experiments. ($^{**}p < 0.01$ and $^{***}p < 0.001$ vs. control).

Mitochondria play a key role in the regulation of apoptosis, specifically through the release of pro-apoptotic proteins located in the intermembrane space. Proteins of the Bcl-2 family, in turn, are involved in the release of mitochondrial proteins through the permeabilization of the external mitochondrial membrane; while proteins as Bax induce the formation of pores in the mitochondrial membrane, members as Bcl-2 inhibit the permeabilization of this structure (Cosentino and García-Sáez, 2014). The activation of the intrinsic pathway by LQFM064 (**4**)

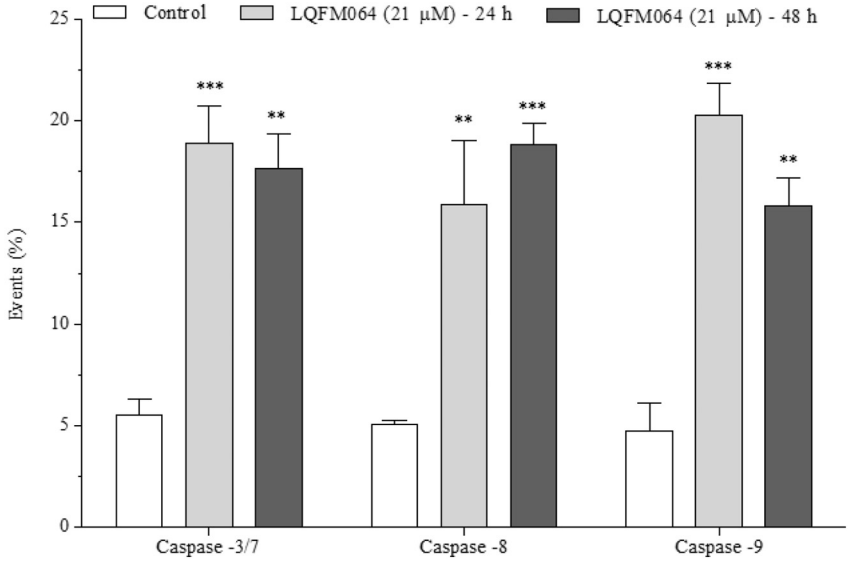


**Fig. 8.** Analysis of caspases − 3/7, − 8 and − 9 activities. The cells ($1 \times 10^5$ cells/mL) were seeded overnight and then treated with or without LQFM064 (**4**) (21 μM) for 24 and 48 h. After treatment, the cells were analyzed using a flow cytometer. Each bar presents mean ± SD of three independent experiments. ($^{**}p < 0.01$ and $^{***}p < 0.001$ vs. control).

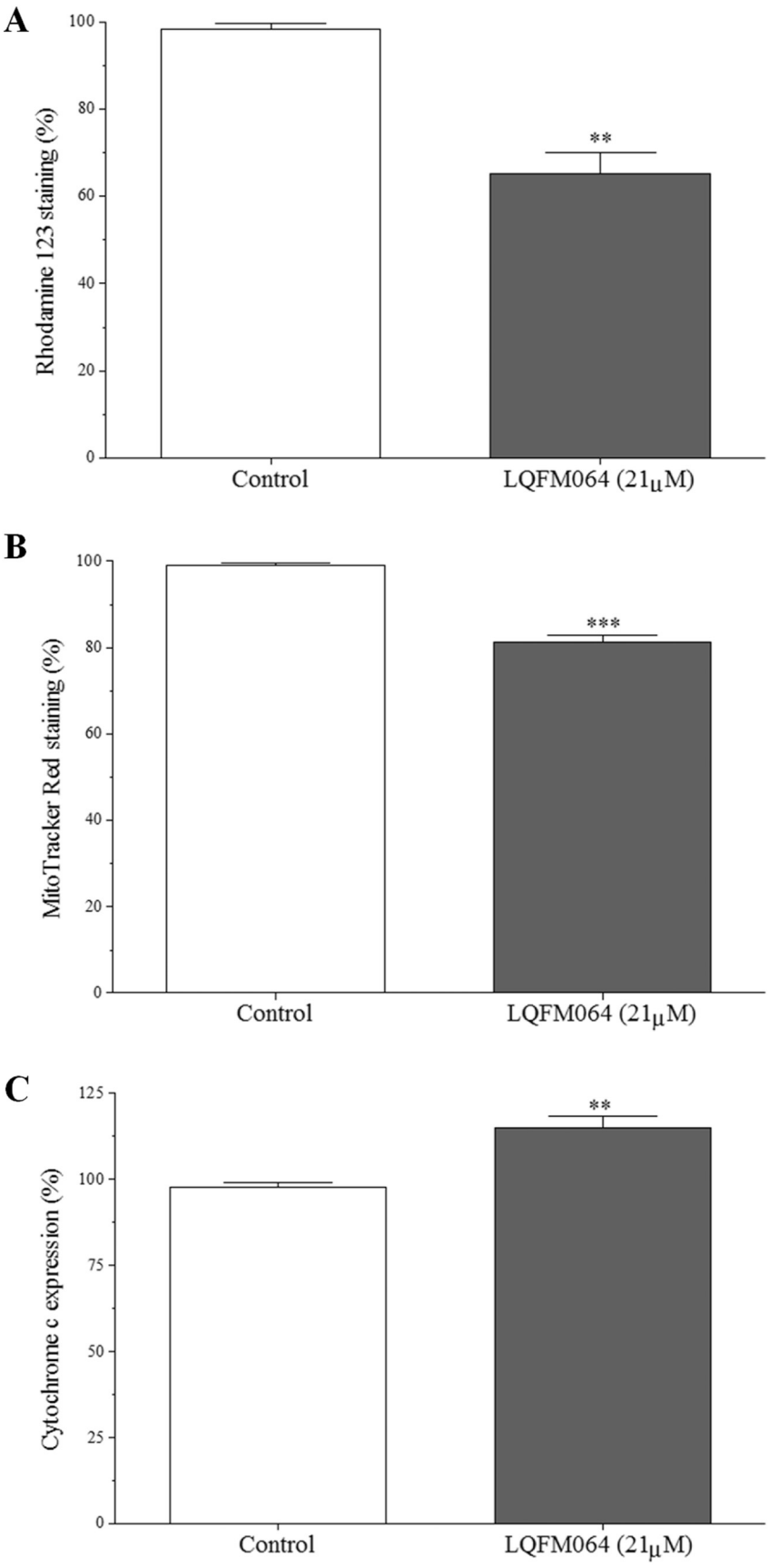


**Fig. 9.** Mitochondrial function analysis of MCF7 cells treated with LQFM064 (**4**). The cells ($1 \times 10^5$ cells/mL) were seeded overnight and then treated with or without LQFM064 (**4**) (21 μM) for 24 h. Mitochondrial function was analyzed as follows: (A) mitochondrial transmembrane potential (ΔΨm) changes by rhodamine 123 staining, (B) Mitotracker Red staining and (C) cytochrome *c* release from mitochondria to cytosol. Each bar presents mean ± SD of three independent experiments. ($^{**}p < 0.01$ and $^{***}p < 0.001$ vs. control). (For interpretation of the references to colour in this figure legend, the reader is referred to the web version of this article.)

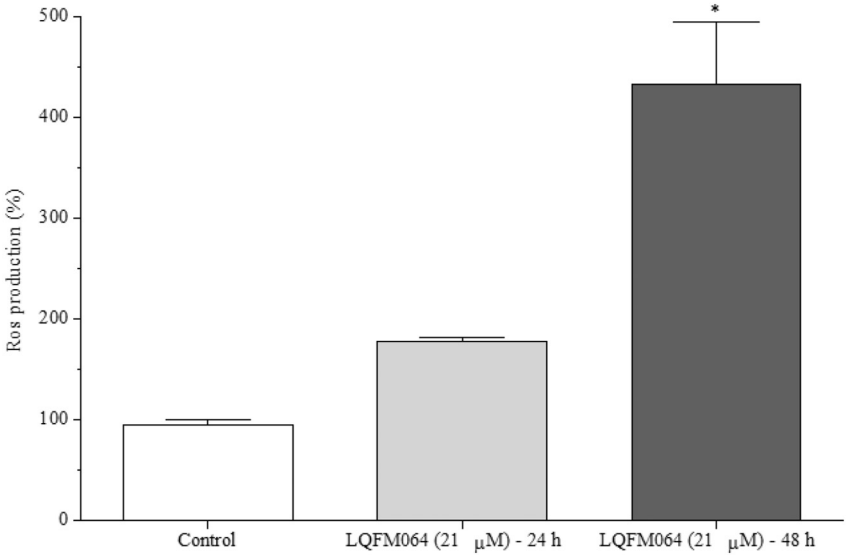


**Fig. 10.** Effects of LQFM064(**4**) treatment of MCF7 cells in ROS generation. The cells ($1 \times 10^5$ cells/mL) were seeded overnight and then treated with or without LQFM064 (**4**) (21 μM) for 24 and 48 h. The cells were then incubated with a fluorimetric probe, 2,7-dichlorodihydrofluorescein diacetate (DCFH-DA), and analyzed by flow cytometer. Each bar presents mean ± SD of three independent experiments. ($^*p < 0.05$ vs. control).

was corroborated through analysis of mitochondrial function, which showed dissipation of the mitochondrial membrane potential. In addition, other results point to the activation of this pathway, such as an increase in cytochrome *c* release and the modulation of proteins of the Bcl-2 family with an increase of Bax and a decrease of Bcl-2 expression.

Reports have shown well-established data of mitochondrial alterations after exposure to chalcone analogues. A study conducted using L1210 leukemic cells showed increased Bax and cytochrome *c* and reduced Bcl-2 after treatment with naphthylchalcones (Winter et al., 2014). In addition, other studies have reported a reduction in MMP in response to compounds of this class (Champelovier et al., 2013; Sharma et al., 2010).

During the mitochondrial pathway, mitochondrial membrane potential perturbation leads to ROS overproduction, and culminates in the development of a potentially cytotoxic state of oxidative stress (Kardeh et al., 2014), as observed here by action of LQFM064 (**4**) in MCF7 cells. As regards the promotion of oxidative stress by chalcone analogues, this condition has been reported in a study by Winter et al. (2010) in which treatment with three distinct naphthylchalcones led to dissipation of membrane potential, increased levels of ROS and reduced ATP in the

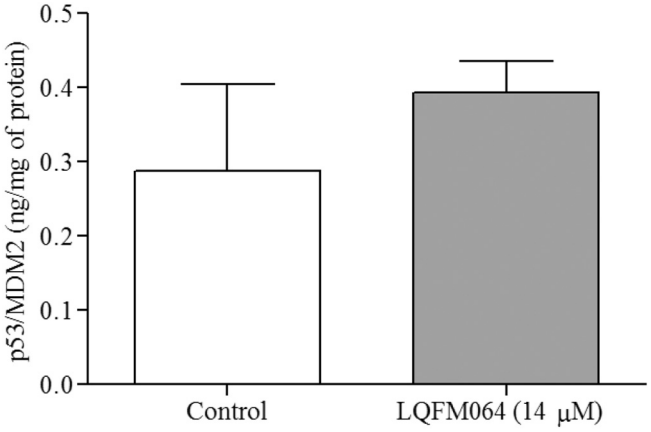


**Fig. 12.** Effects of LQFM064 (**4**) in formation of p53/MDM2 complex in MCF7 cells. The cells ($1 \times 10^4$ cells/well) were seeded and treated with or without LQFM064 (**4**) (14 μM) for 48 h. The cell lysates were then obtained to carry out the analysis. Each bar presents mean ± SD of two independent experiments.

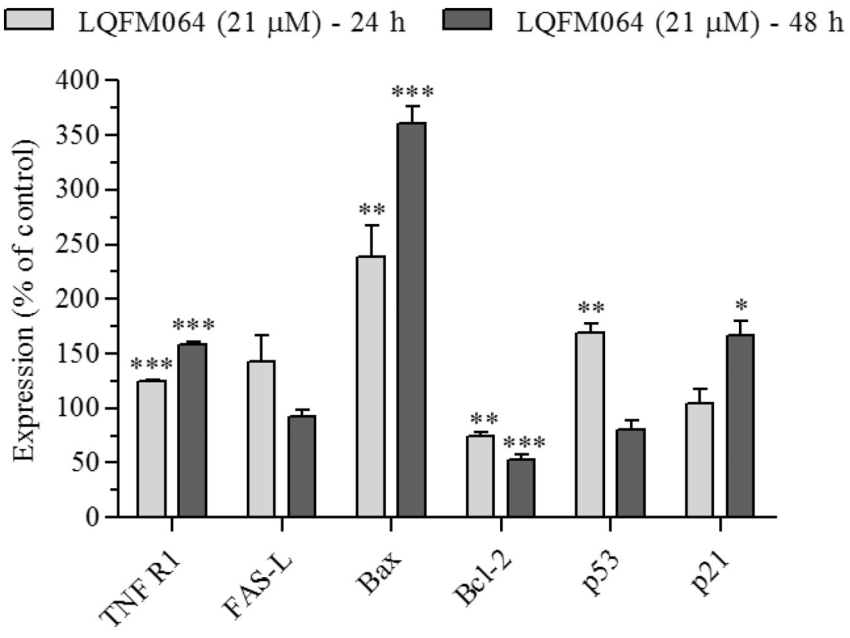


**Fig. 11.** Effects of LQFM064 (**4**) in proteins involved in the process of apoptosis of MCF7 cells. The cells ($1 \times 10^5$ cells/mL) were seeded overnight and then treated with or without LQFM064 (**4**) (21 μM) for 24 and 48 h. After that, analyzes of TNF-R1(A), Fas-L (B), Bax (C), Bcl-2 (D), p53 (E) and p21 (F) expressions were performed by flow cytometer. Each bar presents mean ± SD of three independent experiments. ($^*p < 0.05$, $^{**}p < 0.01$ and $^{***}p < 0.001$ vs. control).

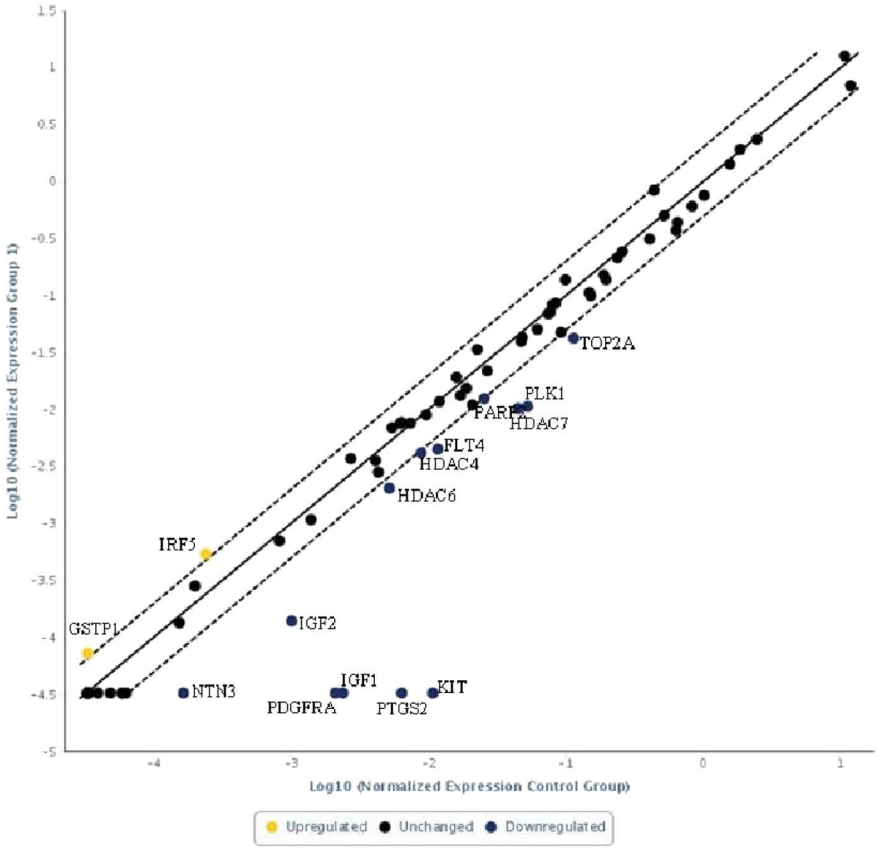


**Fig. 13.** Gene expression changes triggered by LQFM064 (**4**) in MCF7 cells. The cells ($1 \times 10^5$ cells/mL) were treated with or without LQFM064 (**4**) (14 μM) for 48 h. The RNA was then isolated to carry out the gene expression array analysis. Data are representative of two independent experiments.

L1210 leukemic cell line.

Although most existing chemotherapeutic agents induce apoptosis via the intrinsic pathway, the activation of both pathways has been reported and represents advantages (Nakata et al., 2004; Ray and Almasan, 2003; Winter et al., 2014). This present study showed the possible activation of the extrinsic pathway through increased expression of caspase-8, as well as, TNF-R1, Fas-L and as previously mentioned mitochondrial dysfunction. Considering that cancer cells, including breast cancer, usually become resistant to conventional chemotherapy, new drugs such as LQFM64 (**4**) with distinct molecular mechanism of cell death are need. In this sense, Mai et al. (2014) reported increased expression of TNF-R1 in HT-29 colorectal carcinoma cell line in response to treatment with chalcone derivatives. Still on the effects of synthetic chalcone-like compounds, Hsu et al. (2006) reported positive modulation in Fas-L expression in MCF7 and MDA-MB-231 cells.

Several antitumor agents are known to exert inhibitory effects on tumor growth by inducing cell cycle arrest and apoptosis. In results

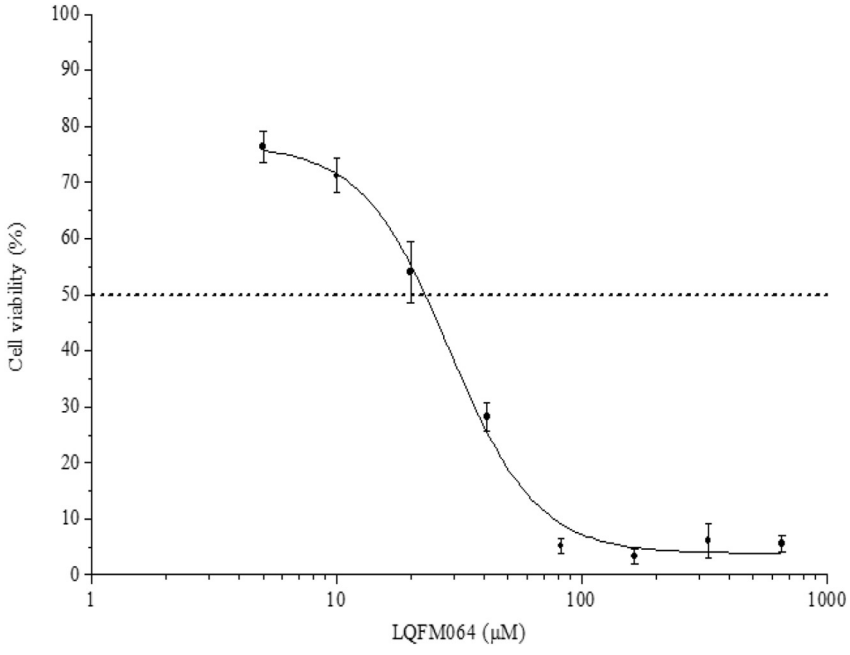


**Fig. 14.** Cytotoxicity evaluation of LQFM064 (**4**) in 3T3 fibroblasts. The cells ($3 \times 10^4$ cells/well) were seeded overnight and then treated with or without different concentrations of LQFM064 (**4**) (5–655 μM) for 48 h. After that, cell viability was evaluated using neutral red uptake (NRU) assay. Each point presents mean ± SD of three independent experiments. (For interpretation of the references to colour in this figure legend, the reader is referred to the web version of this article.)

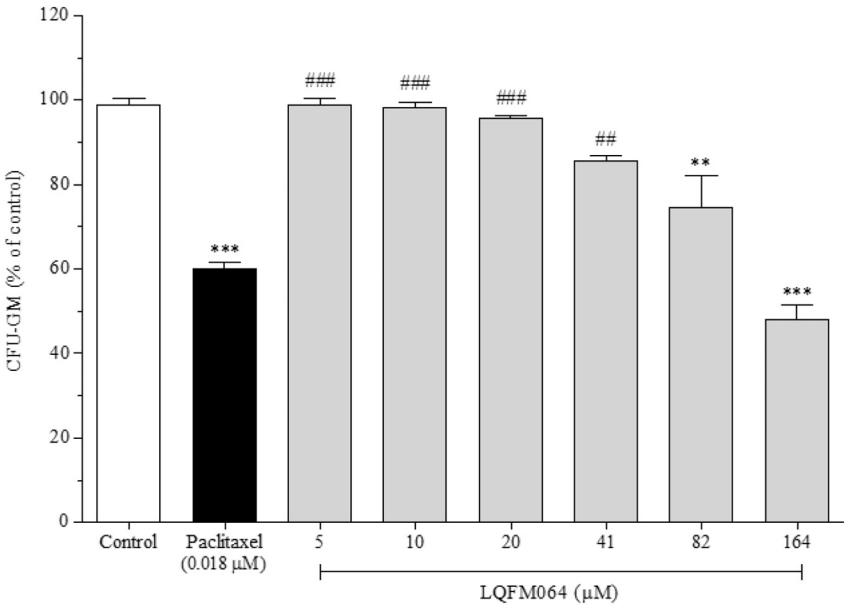


**Fig. 15.** Evaluation of potential myelototixicity of LQFM064(**4**) in mouse bone marrow cells. The cells were collected from a mouse and treated with or without six different concentrations of LQFM064 (**4**) (5–164 μM) for 7 days. After incubation, colony forming units-granulocyte/macrophage (CFU-GM) were scored. Each bar presents mean ± SD of three independent experiments. ($^{**}p < 0.01$ and $^{***}p < 0.001$ vs. control; $^{\#\#}p < 0.01$ and $^{\#\#\#}p < 0.001$ vs. paclitaxel).

similar to ours, Mohamed et al. (2014) showed an increase in the percentage of MCF7 cells at G0/G1 phase after treatment with synthetic chalcone analogues containing pyrazole ring. The inhibitory action exerted by LQFM064 (**4**) on the cell cycle appears to occur as a result of the positive modulation of specific proteins. Under cell stress conditions, p53 positively modulates p21. In turn, p21 exerts inhibitory activity on CDK, thereby preventing progression of the cell cycle through the detection of DNA damage. In addition, this protein interacts directly with other transcription factors, by acting as an inducer of senescence or apoptosis (Dotto, 2000; Ferrándiz et al., 2012). Thus, corroborating the results obtained in the cell cycle analysis, the treatment with LQFM064 (**4**) led to an increase on the expressions of the p53 and p21 proteins, and culminated with the resultant cell cycle arrest.

It has been shown that the modulation of p53 and p21 associated with inhibition of Bcl-2 and increased ROS indicate a possible activation of the p53 pathway (Pietenpol and Stewart, 2002). Thus, the aforementioned results suggest that LQFM064 (**4**) appears to act via this pathway. However, as the intracellular levels of the p53-MDM2 complex were not significantly altered by the treatment, it can be stated that the compound activates the p53 pathway, irrespective of the direct effect on the complexation with its MDM2 inhibitor.

Leão et al. (2015) investigated the molecular mechanisms involved in the antitumoral action of two phenylchalcones and showed that the compounds evaluated were cytotoxic against HCT116 colon adenocarcinoma cells through activation of the p53 pathway, by means of the positive modulation of the p53 and p21 proteins and the reduction in Bcl-2 levels.

KIT and PDGFRA are attractive targets since the tyrosine kinase receptors regulate several essential functions in normal cells. However, overexpression or mutation of these genes are associated with tumorigenesis and cell proliferation, in particular in breast cancer (Carvalho et al., 2005; Hines et al., 1995; Hojjat-Farsangi, 2014; Hsu and Hung, 2016). In this respect, Zhu et al. (2014) demonstrated that 42.1% of triple negative breast cancer, which has higher grade and a poor prognosis in young patients, expresses c-kit protein. These authors identified c-kit as a hot therapeutic target for cancer treatment using tyrosine kinase inhibitors, such as imatinib. This drug is a selective inhibitor of receptor tyrosine kinase, including PDGFR-β and c-kit. Recently, Kadivar et al. (2017) demonstrated antiproliferative effect, apoptosis induction and cytostatic activity of imatinibe in MCF7 cells via PDGFR-β, PDGF-BB, c-Kit and SCF genes modulation.

It is well known that IGF1, an insulin-like growth factor, suppresses apoptosis and promote cell cycle progression, angiogenesis and metastatic activities in various cancers. Thus, blocking the overexpression of this key regulator of tumor development is a positive result for the treatment of breast cancer (Kang et al., 2012; Pacher et al., 2007; Werner and Bruchim, 2012). Considering that tyrosine kinase receptors and insulin-like growth factors are targets of cytotoxic effect of LQFM064 (**4**) in MCF7 cells, we suggest the modulation of these genes are involved in the apoptotic process triggered by this compound.

Furthermore, LQFM064 (**4**) promoted an increase of GSTP1 and IRF5 gene expressions. GSTP1 is involved in drug metabolism and IRF5 is a transcription factor that is critical as immune regulator. IRF5 regulates multiple cellular processes involved in the conversion of normal mammary epithelial cells to tumor epithelial cells with metastatic potential and is lost in ~80% of invasive ductal carcinomas examined (Bi et al., 2011; Pimenta et al., 2015). Altogether, LQFM064 (**4**) has the potential to interfere with important target drug genes.

In vitro methods are widely used as screening in the evaluation of toxicity during the early stages of the development of a new drug candidate (Eisenbrand et al., 2002). After analysis of the mechanisms of cell death, a brief screening was undertaken in terms of the safety profile of LQFM064 (**4**), through the cytotoxic action in the 3T3 basal cell line and mouse bone marrow hematopoietic progenitor cells. On the basis of the $IC_{50}$ determined for 3T3 cells, the $LD_{50}$ was estimated. According to UN GHS, the $LD_{50}$ obtained was between 300 and 2000 mg/kg, which classifies LQFM064 (**4**) as UN GHS Category 4. Based on this classification, it can be inferred that compound (**4**) has a moderate acute oral systemic toxicity hazard, although in vivo analyzes are needed to corroborate this result. As regards hematotoxicity evaluation, it was seen that LQFM064 (**4**) reduced the viability of mouse bone marrow hematopoietic progenitors in concentration-dependent manner. However, the $IC_{50}$ found was about seven times greater than that determined for MCF7 cells. In addition, LQFM064 (**4**) showed a lower cytotoxicity when compared to paclitaxel, a drug widely used in cancer treatment, including breast cancer. Thus, this chalcone derivative seems to have a reduced potential myelotoxicity.

## 5. Conclusions

Given the above, our results suggest that LQFM064 (**4**) induced apoptosis in MCF7 cells by multi-target cytotoxic mechanisms. The mechanism of action of LQFM064 (**4**) involved inhibiting of cell cycle progression associated with increase caspase activities and p53 and p21

expressions, changes the MMP with modulation of the Bcl-2 family protein, and increased expressions of TNF-R1 and Fas-L. KIT, IGF1, PDGFRA, GSTP1 and IRF5 were also targets of the LQFM064 (**4**)-induced cytotoxic effects in MCF7 cells. Thus, this prototype is a promising alternative for the treatment of neoplasias, especially in terms of the development of drug resistance to some apoptotic pathways. Further studies are necessary to better characterize the pharmaco-toxicological effects of LQFM064 (**4**) to become it a future clinical tool.

## Declaration of Interest

The authors declare no conflict of interest.

## Acknowledgements

This study was supported by Brazilian research funding agencies, such as *Conselho Nacional de Desenvolvimento Científico e Tecnológico* (CNPq), *Financiadora de Estudos e Pesquisas* (FINEP), *Coordenação de Aperfeiçoamento de Pessoal de Nível Superior* (CAPES) and *Fundação de Apoio à Pesquisa da Universidade Federal de Goiás* (FUNAPE).

## Appendix A. Supplementary Data

Supplementary data to this article can be found online at http://dx.doi.org/10.1016/j.ejps.2017.06.018.

## References

Bi, X., Hameed, M., Mirani, N., Pimenta, E.M., Anari, J., Barnes, B.J., 2011. Loss of interferon regulatory factor 5 (IRF5) expression in human ductal carcinoma correlates with disease stage and contributes to metastasis. Breast Cancer Res. 13, R111.
Borenfreund, E., Puerner, J.A., 1985. A simple quantitative procedure using monolayer cultures for cytotoxicity assays (HTD/NR-90). J. Tissue Cult. Methods 9, 7–9.
Carvalho, I., Milanezi, F., Martins, A., Reis, R.M., Schmitt, F., 2005. Overexpression of platelet-derived growth factor receptor α in breast cancer is associated with tumour progression. Breast Cancer Res. 7, R788–R795.
Champelovier, P., Chauchet, X., Hazane-Puch, F., Vergnaud, S., Garrel, C., Laporte, F., Boutonnat, J., Boumendjel, A., 2013. Cellular and molecular mechanisms activating the cell death processes by chalcones: critical structural effects. Toxicol. in Vitro 27, 2305–2315.
Cosentino, K., García-Sáez, A.J., 2014. Mitochondrial alterations in apoptosis. Chem. Phys. Lipids 181, 62–75.
Dotto, G.P., 2000. p21WAF1/Cip1: more than a break to the cell cycle? Biochim. Biophys. Acta 1471, M43–M56.
Echeverria, C., Santibañez, J.F., Donoso-Tauda, O., Escobar, C.A., Ramirez-Tagle, R., 2009. Structural antitumoral activity relationships of synthetic chalcones. Int. J. Mol. Sci. 10, 221–231.
Eisenbrand, G., Pool-Zobel, B., Baker, V., Balls, M., Blaauboer, B.J., Boobis, A., Carere, A., Kevekordes, S., Lhuguenot, J.C., Pieters, R., Kleiner, J., 2002. Methods of *in vitro* toxicology. Food Chem. Toxicol. 40, 193–236.
Farrugia, L., 2012. WinGX and ORTEP for windows: an update. J. Appl. Crystallogr. 45, 849–854.
Ferlay, J., Soerjomataram, I., Dikshit, R., Eser, S., Mathers, C., Rebelo, M., Parkin, D.M., Forman, D., Bray, F., 2015. Cancer incidence and mortality worldwide: sources, methods and major patterns in GLOBOCAN 2012. Int. J. Cancer 136, E359–E386.
Ferrándiz, N., Caraballo, J.M., García-Gutierrez, L., Devgan, V., Rodriguez-Paredes, M., Lafita, M.C., Bretones, G., Quintanilla, A., Muñoz-Alonso, M.J., Blanco, R., Reyes, J.C., Agell, N., Delgado, M.D., Dotto, G.P., León, J., 2012. p21 as a transcriptional co-repressor of S-phase and mitotic control genes. PLoS One 7, e37759.
Gonzalez-Angulo, A., Morales-Vasquez, F., Hortobagyi, G., 2007. Overview of resistance to systemic therapy in patients with breast cancer. Adv. Exp. Med. Biol. 608, 1–22.
Harvey, A.L., 2008. Natural products in drug discovery. Drug Discov. Today 13, 894–901.
Hines, S., Organ, C., Kornstein, M., Krystal, G., 1995. Coexpression of the c-kit and stem cell factor genes in breast carcinomas. Cell Growth Differ. 6, 769–779.
Hojjat-Farsangi, M., 2014. Small-molecule inhibitors of the receptor tyrosine kinases: promising tools for targeted cancer therapies. Int. J. Mol. Sci. 15, 13768–13801.
Hsu, J.L., Hung, M.-C., 2016. The role of HER2, EGFR, and other receptor tyrosine kinases in breast cancer. Cancer Metastasis Rev. 35, 575–588.
Hsu, Y.L., Kuo, P.L., Tzeng, W.S., Lin, C.C., 2006. Chalcone inhibits the proliferation of human breast cancer cell by blocking cell cycle progression and inducing apoptosis. Food Chem. Toxicol. 44, 704–713.
ICCVAM, 2006. Test method evaluation report (TIMER): *In vitro* Cytotoxicity Test Methods for Estimating Starting Doses for Acute Oral Systemic Toxicity Test. NIH Publication No. 07-4519. National Institute for Environmental Health Sciences, Research Triangle Park, NC.
Jandial, D.D., Blair, C.A., Zhang, S., Krill, L.S., Zhang, Y.-B., Zi, X., 2014. Molecular targeted approaches to cancer therapy and prevention using chalcones. Curr. Cancer Drug Targets 14, 181–200.
Jänicke, R.U., 2009. MCF-7 breast carcinoma cells do not express caspase-3. Breast Cancer Res. Treat. 117, 219–221.
Kadivar, A., Kamalidehghan, B., Akbari Javar, H., Karimi, B., Sedghi, R., Noordin, M.I., 2017. Antiproliferation effect of imatinib mesylate on MCF7, T-47D tumorigenic and MCF 10A nontumorigenic breast cell lines via PDGFR-β, PDGF-BB, c-Kit and SCF genes. Drug Des. Dev. Ther. 11, 469–481.
Kang, H.J., Yi, Y.W., Kim, H.J., Hong, Y.B., Seong, Y.S., Bae, I., 2012. BRCA1 negatively regulates IGF-1 expression through an estrogen-responsive element-like site. Cell Death Dis. 3, e336.
Kardeh, S., Ashkani-Esfahani, S., Alizadeh, A.M., 2014. Paradoxical action of reactive oxygen species in creation and therapy of cancer. Eur. J. Pharmacol. 735, 150–168.
Leão, M., Soares, J., Gomes, S., Raimundo, L., Ramos, H., Bessa, C., Queiroz, G., Domingos, S., Pinto, M., Inga, A., Cidade, H., Saraiva, L., 2015. Enhanced cytotoxicity of prenylated chalcone against tumour cells via disruption of the p53–MDM2 interaction. Life Sci. 142, 60–65.
Lee, D.H., Jung Jung, Y., Koh, D., Lim, Y., Lee, Y.H., Shin, S.Y., 2016. A synthetic chalcone, 2′-hydroxy-2,3,5′-trimethoxychalcone triggers unfolded protein response-mediated apoptosis in breast cancer cells. Cancer Lett. 372, 1–9.
Mahapatra, D.K., Bharti, S.K., Asati, V., 2015. Anti-cancer chalcones: structural and molecular target perspectives. Eur. J. Med. Chem. 98, 69–114.
Mai, C.W., Yaeghoobi, M., Abd-Rahman, N., Kang, Y.B., Pichika, M.R., 2014. Chalcones with electron-withdrawing and electron-donating substituents: anticancer activity against TRAIL resistant cancer cells, structure–activity relationship analysis and regulation of apoptotic proteins. Eur. J. Med. Chem. 77, 378–387.
Maioral, M.F., Gaspar, P.C., Rosa Souza, G.R., Mascarello, A., Chiaradia, L.D., Licínio, M.A., Moraes, A.C.R., Yunes, R.A., Nunes, R.J., Santos-Silva, M.C., 2013. Apoptotic events induced by synthetic naphthylchalcones in human acute leukemia cell lines. Biochimie 95, 866–874.
Mohamed, M., Mohamed, M., Fathi, M., Shouman, S., Abdelhamid, I., 2014. Chalcones incorporated pyrazole ring inhibit proliferation, cell cycle progression, angiogenesis and induce apoptosis of MCF7 cell line. Anti Cancer Agents Med. Chem. 14, 1282–1292.
Mosmann, T., 1983. Rapid colorimetric assay for cellular growth and survival: application to proliferation and cytotoxicity assays. J. Immunol. Methods 65, 55–63.
Nakata, S., Yoshida, T., Horinaka, M., Shiraishi, T., Wakada, M., Sakai, T., 2004. Histone deacetylase inhibitors upregulate death receptor 5//TRAIL-R2 and sensitize apoptosis induced by TRAIL//APO2-L in human malignant tumor cells. Oncogene 23, 6261–6271.
Nounou, M.I., ElAmrawy, F., Ahmed, N., Abdelraouf, K., Goda, S., Syed-Sha-Qhattal, H., 2015. Breast cancer: conventional diagnosis and treatment modalities and recent patents and technologies. Breast Cancer (Auckl.) 9, 17–34.
Pacher, M., Seewald, M.J., Mikula, M., Oehler, S., Mogg, M., Vinatzer, U., Eger, A., Schweifer, N., Varecka, R., Sommergruber, W., Mikulits, W., Schreiber, M., 2007. Impact of constitutive IGF1/IGF2 stimulation on the transcriptional program of human breast cancer cells. Carcinogenesis 28, 49–59.
Park, C.-S., Ahn, Y., Lee, D., Moon, S.W., Kim, K.H., Yamabe, N., Hwang, G.S., Jang, H.J., Lee, H., Kang, K.S., Lee, J.W., 2015. Synthesis of apoptotic chalcone analogues in HepG2 human hepatocellular carcinoma cells. Bioorg. Med. Chem. Lett. 25, 5705–5707.
Pessina, A., Albella, B., Bueren, J., Brantom, P., Casati, S., Gribaldo, L., Croera, C., Gagliardi, G., Foti, P., Parchment, R., Parent-Massin, D., Sibiril, Y., Van Den Heuvel, R., 2001. Prevalidation of a model for predicting acute neutropenia by colony forming unit granulocyte/macrophage (CFU-GM) assay. Toxicol. in Vitro 15, 729–740.
Pietenpol, J.A., Stewart, Z.A., 2002. Cell cycle checkpoint signaling: cell cycle arrest versus apoptosis. Toxicology 181–182, 475–481.
Pimenta, E.M., De, S., Weiss, R., Feng, D., Hall, K., Kilic, S., Bhanot, G., Ganesan, S., Ran, S., Barnes, B.J., 2015. IRF5 is a novel regulator of CXCL13 expression in breast cancer that regulates CXCR5 + B- and T-cell trafficking to tumor-conditioned media. Immunol. Cell Biol. 93, 486–499.
Ray, S., Almasan, A., 2003. Apoptosis induction in prostate cancer cells and xenografts by combined treatment with Apo2 ligand/tumor necrosis factor-related apoptosis-inducing ligand and CPT-11. Cancer Res. 63, 4713–4723.
Sharma, A., Chakravarti, B., Gupt, M.P., Siddiqui, J.A., Konwar, R., Tripathi, R.P., 2010. Synthesis and anti breast cancer activity of biphenyl based chalcones. Bioorg. Med. Chem. 18, 4711–4720.
Sheldrick, G.M., 2015. Crystal structure refinement with SHELXL. Acta Crystallogr. C Struct. Chem. 71, 3–8.
Siegel, R.L., Miller, K.D., Jemal, A., 2016. Cancer statistics. CA Cancer J. Clin. 66, 7–30.
Singh, P., Anand, A., Kumar, V., 2014. Recent developments in biological activities of chalcones: a mini review. Eur. J. Med. Chem. 85, 758–777.
de Vasconcelos, A., Campos, V.F., Nedel, F., Seixas, F.K., Dellagostin, O.A., Smith, K.R., de Pereira, C.M.P., Stefanello, F.M., Collares, T., Barschak, A.G., 2013. Cytotoxic and apoptotic effects of chalcone derivatives of 2-acetyl thiophene on human colon adenocarcinoma cells. Cell Biochem. Funct. 31, 289–297.
Velaei, K., Samadi, N., Barazvan, B., Soleimani, R., 2016. Tumor microenvironment-mediated chemoresistance in breast cancer. Breast 30, 92–100.
Vieira, M.S., de Oliveira, V., Lima, E.M., Kato, M.J., Valadares, M.C., 2011. *In vitro* basal cytotoxicity assay applied to estimate acute oral systemic toxicity of grandisin and its major metabolite. Exp. Toxicol. Pathol. 63, 505–510.
Werner, H., Bruchim, I., 2012. IGF-1 and BRCA1 signalling pathways in familial cancer. Lancet Oncol. 13, e537–e544.
Winter, E., Chiaradia, L.D., de Cordova, C.A.S., Nunes, R.J., Yunes, R.A., Creczynski-Pasa, T.B., 2010. Naphthylchalcones induce apoptosis and caspase activation in a leukemia cell line: the relationship between mitochondrial damage, oxidative stress, and cell death. Bioorg. Med. Chem. 18, 8026–8034.
Winter, E., Chiaradia, L.D., Silva, A.H., Nunes, R.J., Yunes, R.A., Creczynski-Pasa, T.B., 2014. Involvement of extrinsic and intrinsic apoptotic pathways together with endoplasmic reticulum stress in cell death induced by naphthylchalcones in a leukemic cell line: advantages of multi-target action. Toxicol. in Vitro 28, 769–777.
Zhu, Y., Wang, Y., Guan, B., Rao, Q., Wang, J., Ma, H., Zhang, Z., Zhou, X., 2014. C-kit and PDGFRA gene mutations in triple negative breast cancer. Int. J. Clin. Exp. Pathol. 7, 4280–4285.